A CLASS OF RC-ACTIVE BIQUADRATIC FILTERS DESIGNED WITH RIORDAN'S GENERALISED IMPEDANCE CONVERTER

PETER ANDI-NIBA TAYUKA

A Research Thesis

in

The Faculty

of

Engineering

Presented in Partial Fulfillment of the Requirement
for the degree of Master of Engineering at
Concordia University
Montréal, Québec, Canada

April, 1976

ABSTRACT

PETER ANDI-NIBA TAYUKA

A CLASS OF RC-ACTIVE BIQUADRATIC FILTERS DESIGNED WITH RIORDAN'S GENERALISED IMPEDANCE CONVERTER

Biquadratic active filter sections such as low-pass, high-pass, band-pass, all-pass and notch are derived from Riordan's Generalised Impedance Converter embeded in a simple passice RC structure. These derived sections exhibit high input impedances and, with the exception of the notch section, low output impedances. The sections are shown to be stable during activation.

The sensitivities to passive element variations are found to be low. The pole frequency, ω_0, sensitivity to amplifier dc gain, A_0, is found to be practically negligible. A design procedure which minimizes the sensitivity of pole Q-factor, Q_p, to A_0 variations is given. A tuning procedure, using two resistors per section to adjust ω_0 and Q_p, is described.

The finite gain-bandwidth product of amplifiers, while giving rise to Q_p enhancement, has a negligible effect on ω_0.

Finally, the behaviour of the filters as predicted by the analytical expressions derived in the thesis are confirmed by computer simulation and experimental results.

to the memory of

my grandmother

Nemo Ngum Fru Ma-Che

ACKNOWLEDGEMENTS

The author is deeply indebted to Dr. M.N.S. Swamy for his guidance, supervision and suggestions during the course of this work.

Great appreciation is extended to Dr. A. Antoniou for suggestions on computer simulation programs used in this study. Thanks are due to Dr. B.B. Bhattacharyya for his many useful discussions and for going through the manuscript.

This study was supported under the National Research Council of Canada Grant No. 7739 awarded to Dr. M.N.S. Swamy.

TABLE OF CONTENTS

LIST OF TABLES

LIST OF FIGURES

NOMENCLATURE

A	Operational amplifier gain
A_0	Operational amplifier d.c. gain
AP	All-pass
a_i	Coefficient of s^i in N(s) of second-order transfer function
B	Gain bandwidth product
BP	Band-pass
b_i	Coefficient of s^i in D(s) of second-order transfer function
C	Capacitance of a capacitor
C_{max}	Maximum capitance
C_{min}	Minimum capacitance
D(s)	Denominator of T(s)
f_0	Pole resonant frequency in hertz
G	Conductance of a resistor
GIC	Generalized immitance converter
HP	High-pass
h(s)	Conversion function of GIC
LP	Low-pass
N	Notch
N(s)	Numerator of T(s)
Op.Amp.	Differential input single output operational amplifier
P_i	Coefficient of s^i in N(s) of general open circuit voltage transfer function
Q_p	Pole Q-factor
Q_{pa}	Actual pole Q-factor realized when the finite d.c. gain of Op.Amp. is taken into consideration

Q_{pk}	Actual pole Q-factor realized when gain-bandwidth product of Op.Amp. is taken into consideration
Q_z	Zero Q-factor
q_i	Coefficient of s^i in D(s) of general open circuit voltage transfer function
R	Resistance of a resistor
S	Complex frequency variable
S_e^x	Sensitivity of X due to small changes in e
T(s)	Open circuit voltage transfer function
t	Transmission matrix
ω_c	Op.Amp. corner frequency in radius/sec.
ω_n	Notch frequency in radius/sec.
ω_0	Pole resonant frequency in radius/sec.
ω_{0a}	Actual pole resonant frequency realized when the finite d.c. gain of Op.Amp. is taken into consideration
ω_{0k}	Actual pole resonant frequency realized when the finite gain bandwidth product of Op.Amp. is taken into consideration
ω_z	Zero resonant frequency in radius/sec.

CHAPTER I

INTRODUCTION

1.1 GENERAL

RC-active filters are widely used in many areas such as telephone and data communications, precision instruments and control systems. In these applications the filter networks are often characterized by high Q_p and/or low frequencies of operation. With such network characteristics conventional LC realizations become unsuitable due to the bulky size, poor quality and high cost of inductors. In addition to size and weight reduction provided by RC-active networks, system reliability can be increased substantially by taking advantage of integrated circuit (IC) technology. Using this technology a complex RC network can be built on a single chip. Attempts to fabricate good quality inductors with usable values of inductance by IC techniques have not yet been successful [1].

Designing inductorless filter networks, using only RC and active elements offers the circuit designer other advantages as well. He can design RC-active filters to achieve some characteristics which are difficult to achieve or even impossible using RLC filters. RC-active filters can be designed to exhibit very high input impedances and/or extremely low output impedances. High input impedances reduce loading of the signal source. Low output impedances

allow cascading without additional isolating amplifiers between filter sections or even between filter and load. RC-active networks can be designed to provide insertion gain. In some application this is a definite advantage. Since RC-active networks are not limited by the passivity and reprocity properties exhibited by RLC networks, they can be used to realize s-right half plane zeros with considerable ease.

Through careful design, RC-active filters can be made to exhibit low sensitivities to variations in network elements and good stability properties. The active filter designer is becoming more aware of the limitations of practical active and passive components. Such awareness is leading to the development of circuit design methods which minimize the effects of these limitations.

1.2 APPROACHES AND TECHNIQUES IN RC-ACTIVE FILTER DESIGN

There exists an abundance of literature [2] suggesting different RC-active filter design procedures. Within these procedures there are two basic approaches:

(1) The direct realization in which a transfer function of the form

$$T(s) = \frac{P_m s^m + P_{m-1} s^{m-1} + \ldots + P_1 s + P_0}{q_n s^n + q_{n-1} s^{n-1} + \ldots + q_1 s + q_0} \qquad (1.1)$$

$$m \leq n$$

is synthesized directly as a two-port. Techniques for direct synthesis have been discussed in the literature by Antoniou [3], Orchard [4], Bruton [5], etc.

(2) Alternatively, $T(s)$ can be expressed as

$$T(s) = H \cdot T_1(s) \cdot T_2(s) \cdots T_j(s) \quad (1.2)$$

where each $T_j(s)$ is the biquadratic transfer function

$$T_j(s) = \frac{N_j(s)}{b_{j_2}S^2 + b_{j_1}S + b_{j_0}} \quad (1.3)$$

Here $N_j(s)$ is a polynomial of order ≤ 2 determining the type of filter.

Each $T_j(s)$ is then realized independently. The overall network defined by $T(s)$ is constructed by cascading the different second-order filters. If n is odd a first order filter section is also needed.

This approach, classified as the cascade realization approach, offers a number of practical advantages over the direct realization approach. First, post-manufacture adjustments of the network is simpler as each section is isolated from the others. Also, it is possible to design a few second order building blocks with externally controlled characteristics that allow the realization of higher order

transfer functions by cascading the second-order building blocks.

1.3 ACTIVE ELEMENTS IN FILTER DESIGN

The active elements useful in RC-active network design can be classified as finite-gain or infinite-gain control sources, negative impedance converters (NIC), generalized immittance converters (GIC), gyrators and frequency dependent negative resistance (FDNR). All these active elements can be realized using the Operational Amplifier (Op. Amp.). The properties of Op.Amps. and GIC's will be discussed in detail, since they are used in this work.

1.3.1 Operational Amplifiers (Op.Amp.)

The Op.Amp., shown in Figure 1.1, is a non-reciprocal two-port device ideally characterized by a frequency independent infinite gain, infinite input impedance and zero output impedance. From Figure 1.1(c), the idealized Op. Amp. can be precisely defined as

$$V_0 = A(V_2 - V_1),\ A \to \infty,\ I_1 = I_2 = 0 \qquad (1.4)$$

$$V_0 \to 0 \quad \text{when} \quad (V_2 - V_1) \to 0 \qquad (1.5)$$

Equation (1.5) defines what is known as the zero-offset requirement. The ideal Op.Amp. can also be represented by the nullator-norator (Figure 1.1(e)) model as

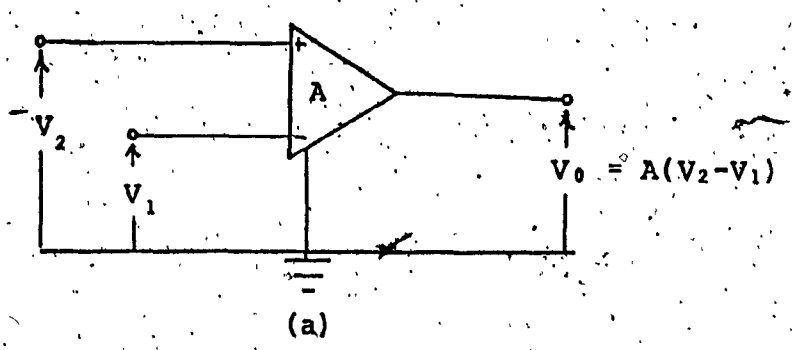

(a)

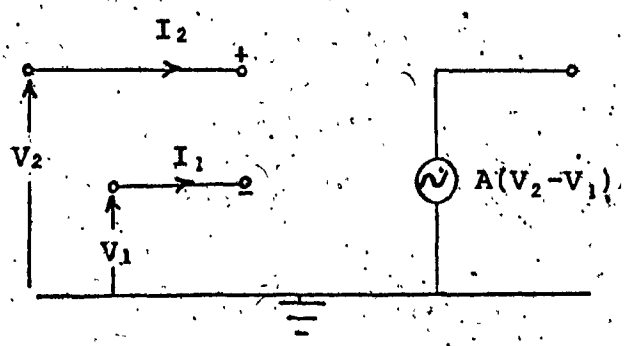

(b)

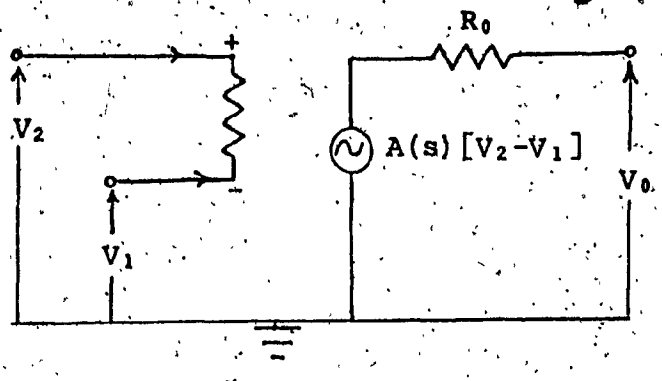

(c)

FIG. 1.1 (a) The Ideal Op.Amp. (Symbolic Representation)

(b) Controlled Source Model of Idealized Op.Amp.

(c) Controlled Source Model of Practical Op.Amp.

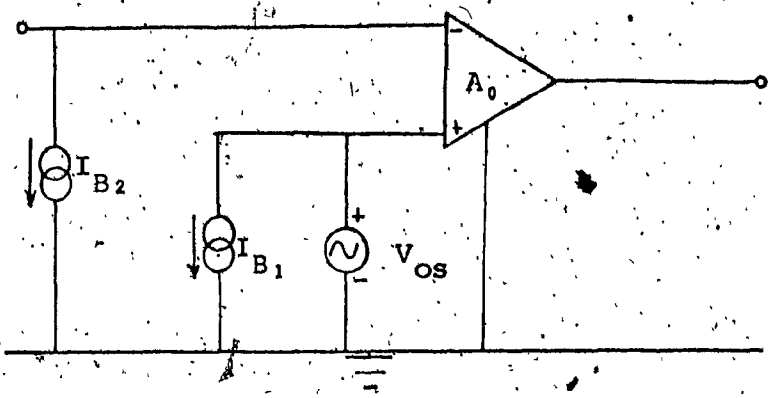

(d)

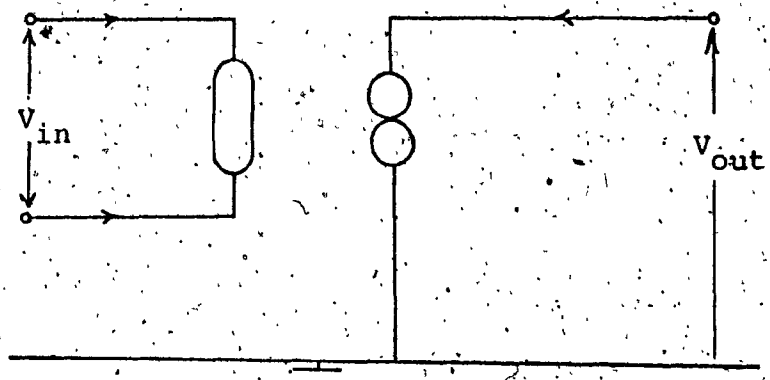

(e)

FIG. 1.1 (cont'd)

(d) Offset Voltage and Bias Currents of Practical Op.Amp.

(e) Nullator-Norator Model of Idealized Op.Amp.

proposed by Mitra [6] and Martinelli [7].

Presently available Op.Amps. have a finite dc voltage gain, input impedance and a non-zero output impedance. For example, the Fairchild μ A741 has a differential input resistance of 2MΩ, output resistance of 75Ω and a dc voltage gain of 200,000. In addition, the gain is frequency dependent. For a frequency compensated Op.Amp., the gain A(s), is given by

$$A(s) = \frac{A_0 \omega_c}{s + \omega_c} = \frac{B}{s + \omega_c} \qquad (1.6)$$

where A_0, ω_c and B are the dc gain, cut-off frequency and gain bandwidth product respectively. A model of the practical Op.Amp. is shown in Figure 1.1(c).

The practical Op.Amp. does not satisfy the condition of zero-offset either. Practical Op.Amps. have dc voltage offsets and bias currents. This offsets drift with time and changing temperature. The effect of these offsets and their drifts may be important in low pass filters used in high precision instruments or in all pass networks where the signal contains information in the sub-audio range. A model for representing these effects is given in Figure 1.1(d).

1.3.2 Generalized Immittance Converters (GIC)

The Generalized Immittance Converter (GIC) is a two-port network where the admittance seen at one of its ports is

a generalized function of the load at the other port. That is

$$Y_i = h(s)Y_L \qquad (1.7)$$

where Y_i is the admittance seen at the input port, Y_L is the load connected at the output port and $h(s)$ is the conversion function. There have been many GIC circuits proposed in the literature [6] which are completely defined by the transmission matrix t, where

$$t = \begin{bmatrix} 1 & 0 \\ 0 & h(s) \end{bmatrix} \qquad (1.8)$$

Figure 1.2 shows two such circuits using nullators and norators. Analysis of these circuits yields

$$h(s) = \frac{Y_1 Y_3}{Y_2 Y_4} \qquad (1.9)$$

To obtain physical networks from the circuits each nullator can be paired up with a norator to give a nullor. The nullor can then be replaced by an Op.Amp. The network that results from Figure 1.2(a) is shown in Figure 1.3(a). This network is due to Antoniou [8]. The circuit of Figure 1.2(b) would yield the network in Figure 1.3(b). This network was originally proposed by Riordan [9] and later modified by Antoniou [10] to render it free from low-frequency unstable modes of operation.

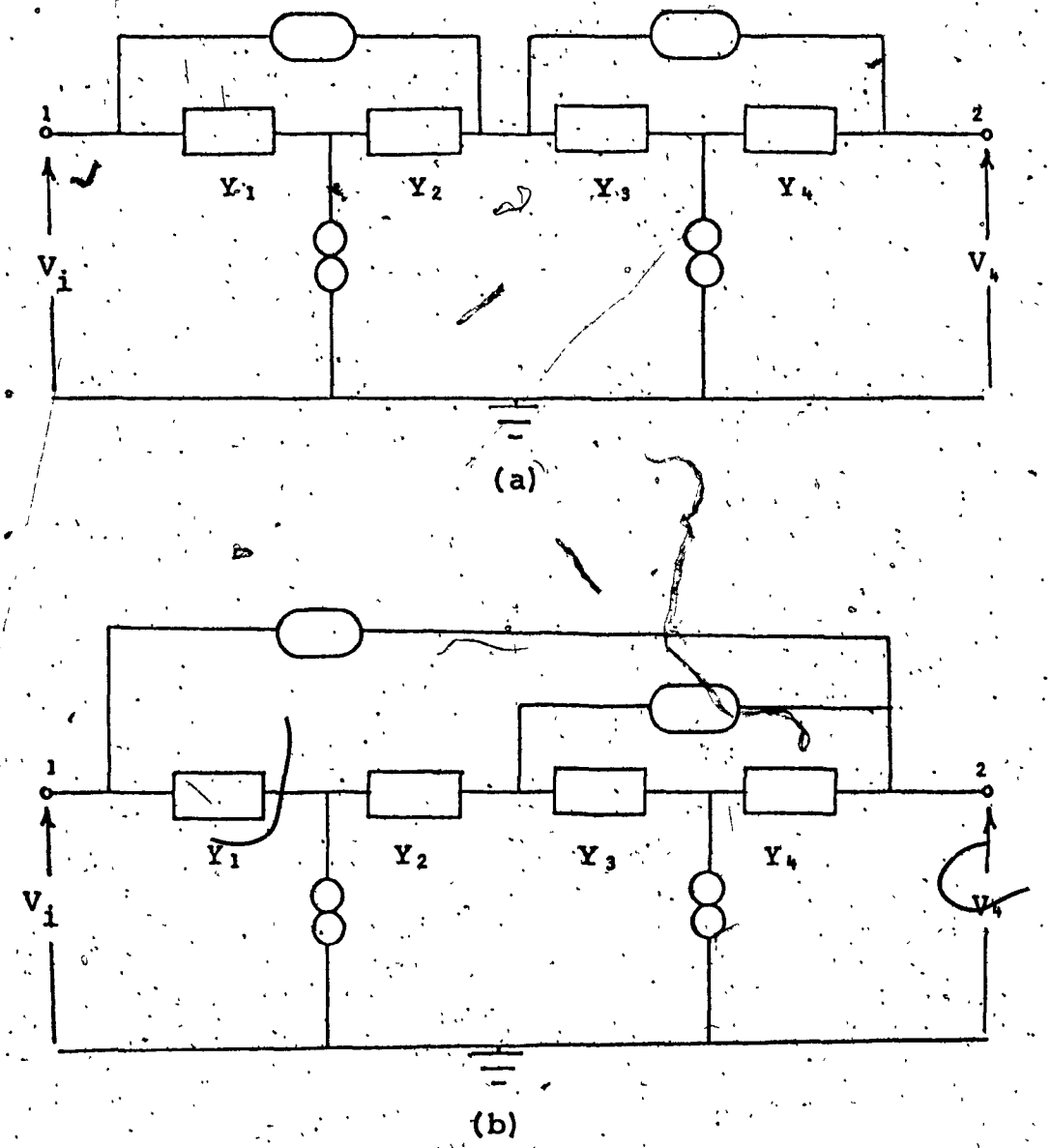

FIG. 1.2 Nullator-Norator Models of GIC's

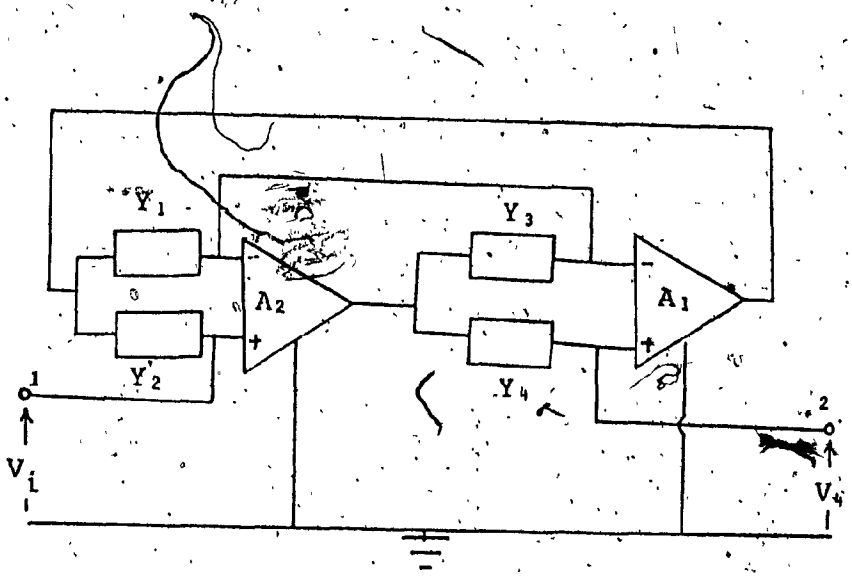

(a)

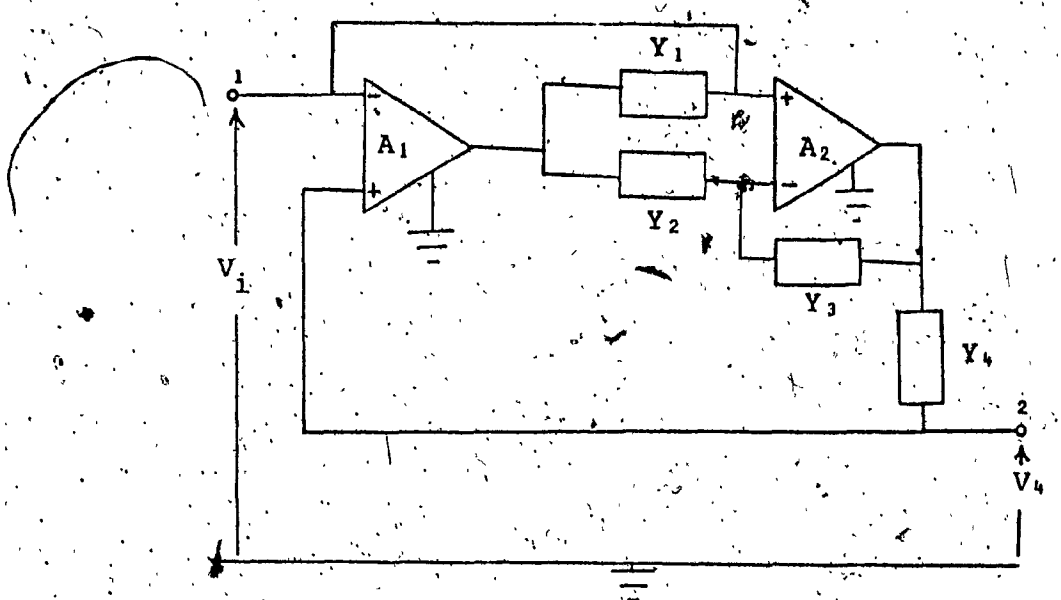

(b)

FIG. 1.3 (a) Antoniou's GIC

(b) Riordan's GIC

1.4 EVALUATION CRITERIA FOR BIQUADRATIC RC-ACTIVE FILTERS

Network parameters such as passive element values, amplifier gains, etc., often exhibit significant variations from their nominal design values. Such variations are usually a result of manufacturing tolerances, changing environmental conditions and component aging. Both elaborate statistical techniques [11,12] and deterministic techniques [6] have been developed to obtain quantitative estimates for the effect of parameter variations on filter performance. While the statistical techniques are more realistic, the deterministic techniques provide a simple but reasonable measure of filter performance under changing conditions.

The general biquadratic transfer function of Eq. (1.3) is characterized by system parameters

$$Q_j \triangleq \sqrt{b_{j0} b_{j2} / b_{j1}} \qquad (1.10a)$$

and

$$\omega_{0j} \triangleq \sqrt{b_{j0} / b_{j2}} \qquad (1.10b)$$

where Q_j is known as the pole Q-factor and ω_{0j} is the pole-frequency.

The two deterministic performance figures of merit most commonly used are the Q-sensitivity and the pole-frequency sensitivity defined as

$$S_e^Q = \frac{\partial Q / Q}{\partial e / e} \qquad (1.11a)$$

and

$$S_e^{\omega_0} = \frac{\partial \omega_0 / \omega_0}{\partial e / e} \qquad (1.11b)$$

where e is the network parameter of interest. Designers strive to keep the sensitivities with respect to the passive and active parameters as low as possible.

Variations of filter response caused by manufacturing tolerances can be eliminated by tuning for the designed Q and ω_0. It becomes necessary then that the filters be easily tunable and the tuning be preferably resistive.

Closely related to the sensitivity problem is the stability problem caused by active element imperfections. It has been shown [8] that there is a distinct possibility of some Op.Amp. filter networks becoming self-oscillatory following activation. Also, the excess phase introduced by the Op.Amp. pole is, in many cases, a source of potential instability. It is thus a necessity that stability properties of each active network be studied in detail.

If the designed filters are to take advantage of IC fabrication technology, it is essential to limit the total capacitance and resistance. The spread in the values of capacitors and resistors should be compatible with IC fabrication techniques.

1.5 STATEMENT OF THE PROBLEM

It has recently been shown that RC-active networks

designed with GIC's exhibit very low sensitivities to element variations. Biquads designed with Antoniou's GIC (Figure 1.3(a)) have been shown to have excellent characteristics [13,14,15].

The purpose of this work is to design biquads using the Riordan's GIC of Figure 1.3(b) and to determine their properties. To this end, Chapter II is concerned with the analysis of Riordan's GIC with the view of deriving biquads from it. The sensitivity properties of the derived biquads are then studied. Using the sensitivity properties a design procedure is then given.

In Chapter III, the effects of Op. Amp. imperfections on the derived biquads are studied. Experimental and simulation results verify the theoretical predictions derived in this chapter. Chapter IV summarizes the study and gives a comparison of these biquads with other biquads.

CHAPTER II

BIQUADRATIC SECTIONS DERIVED FROM RIORDAN'S GIC

2.1 INTRODUCTION

Riordan's GIC (Figure 1.3(b)) is analysed with the gains of the Op. Amps. considered finite and all other Op. Amps. imperfections are negligible. Biquadratic sections are then derived from the GIC by embeding it in a passive double-L structure. Both the active and passive sensitivity of the biquadratic sections are studied and a design procedure that uses the sensitivity properties as constraints is given.

2.2 TRANSMISSION MATRIX OF RIORDAN'S GIC

If the Op.Amps. are considered to have zero input and infinite output admittances the controlled source representation of Riordan's GIC is shown in Figure 2.1.

The nodal equilibrium equations for the network are

$$I_1 = [V_i - A_1(V_4 - V_i)]Y_1 \qquad (2.1a)$$

$$I_2 = [V_4 - A_2(V_i - V_3)]Y_4 \qquad (2.1b)$$

$$0 = [V_3 - A_2(V_4 - V_i)]Y_2 + [V_3 - A_2(V_i - V_3)]Y_2 \qquad (2.1c)$$

From this set of equations the Y-matrix for Riordan's GIC is

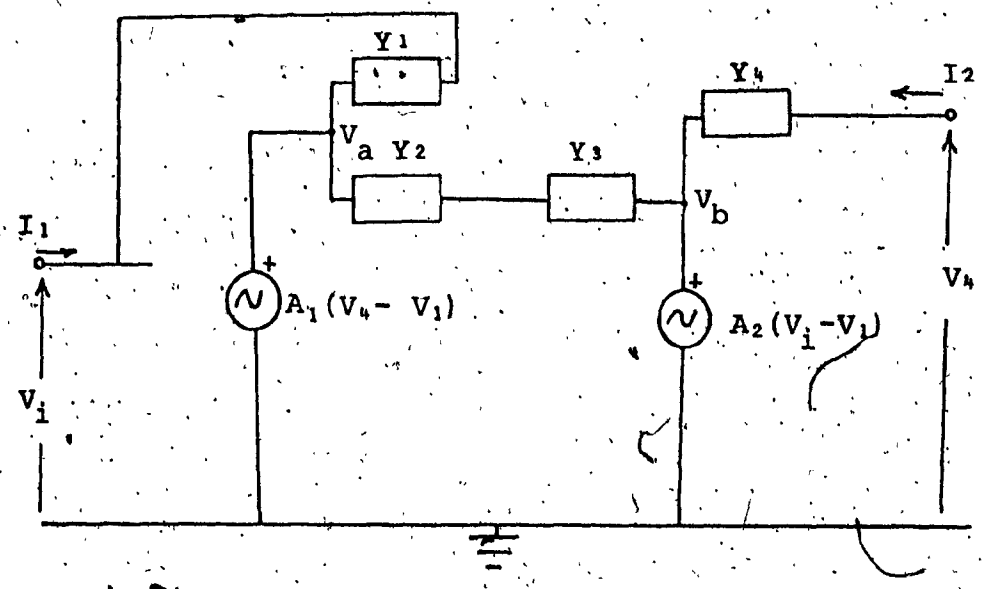

FIG. 2.1 Controlled Source Model of Riordan's GIC

$$Y = \begin{bmatrix} Y_1 + A_1Y_1 & -A_1Y_1 \\ \dfrac{A_2Y_2Y_4 + A_2Y_3Y_4 + A_1A_2Y_2Y_4}{Y_2 + Y_3 + A_2Y_3} & \dfrac{Y_2Y_4 + Y_3Y_4 + A_2Y_3Y_4 + A_1A_2Y_2Y_4}{Y_2 + Y_3 + A_2Y_3} \end{bmatrix} \qquad (2.2)$$

The determinant is

$$\triangle Y = \frac{Y_1Y_2Y_4 + Y_1Y_3Y_4 + A_2Y_1Y_3Y_4 + A_1Y_1Y_2Y_4 + A_1Y_1Y_3Y_4}{Y_2 + Y_3 + A_2Y_3} \qquad (2.3)$$

Given the Y-matrix the transmission matrix, t, is

$$t = \begin{bmatrix} -\dfrac{Y_{22}}{Y_{21}} & -\dfrac{1}{Y_{21}} \\ -\dfrac{\triangle Y}{Y_{21}} & -\dfrac{Y_{11}}{Y_{21}} \end{bmatrix} \qquad (2.4)$$

Thus the transmission matrix for Riordan's GIC is

$$t = \begin{bmatrix} \dfrac{Y_2Y_4(1+A_1A_2) + Y_3Y_4(1+A_2)}{Y_2Y_4(A_2+A_1A_2) + A_2Y_3Y_4} & \dfrac{Y_2 + Y_3(1+A_2)}{Y_2Y_4(A_2+A_1A_2) + A_2Y_3Y_4} \\ \dfrac{Y_1Y_3Y_4(1+A_1+A_2) + Y_1Y_2Y_4(1+A_1)}{Y_2Y_4(A_2+A_1A_2) + A_2Y_3Y_4} & \dfrac{Y_1Y_2(1+A_1) + Y_1Y_3(1+A_1+A_2+A_1A_2)}{Y_2Y_4(A_2+A_1A_2) + A_2Y_3Y_4} \end{bmatrix} \qquad (2.5)$$

In the limiting case (i.e., $A_1, A_2 \to \infty$) the transmission matrix is given by

$$t = \begin{bmatrix} 1 & 0 \\ 0 & \frac{Y_1 Y_3}{Y_2 Y_4} \end{bmatrix} \qquad (2.6)$$

This agrees with the nullator-norator model discussed earlier.

2.3 THE BASIC CONFIGURATION

To obtain biquadratic sections the GIC is embeded in the passive structure containing admittances Y_5, Y_6, Y_7, Y_8 as shown in Figure 2.2(a). The output V_4 is taken across Y_8 while V_a and V_b are obtained at the outputs of the two Op. Amps. within the GIC. This is explicitly shown in Figure 2.2(b).

2.3.1 Analysis of Basic Configuration Using Riordan's GIC

Inspection of Figure 2.2(b) shows that

$$V_a = A_1(V_4 - V_i) \qquad (2.7a)$$

$$V_b = A_2(V_i - V_3) \qquad (2.7b)$$

The nodal equilibrium matrix equation of this network is given as

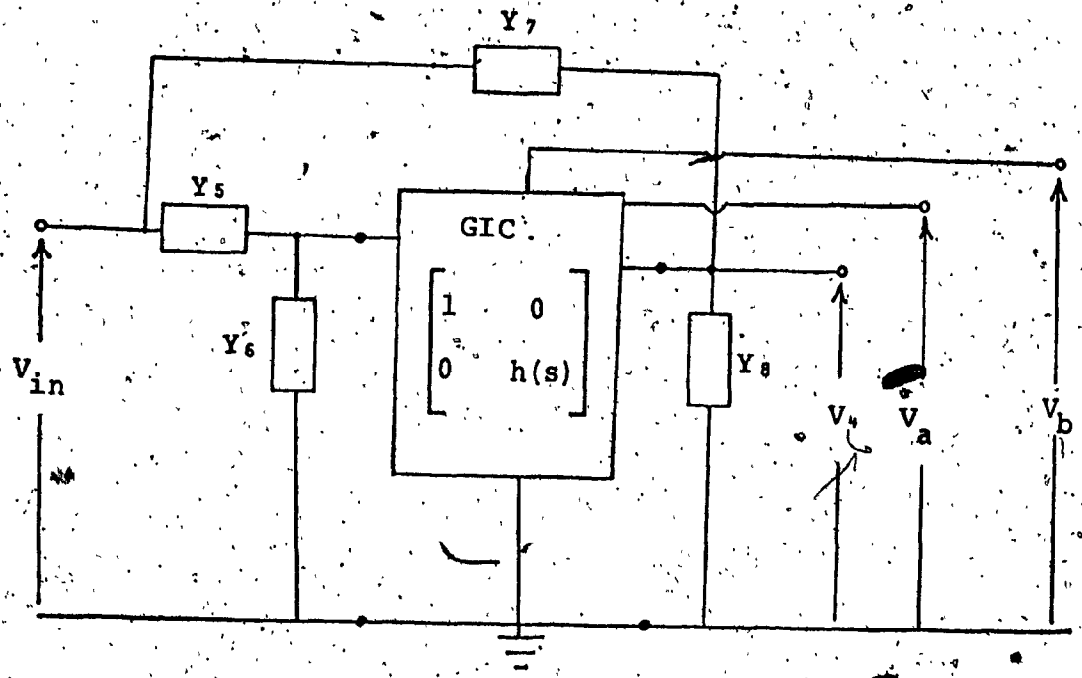

FIG. 2.2 (a) Basic Structure

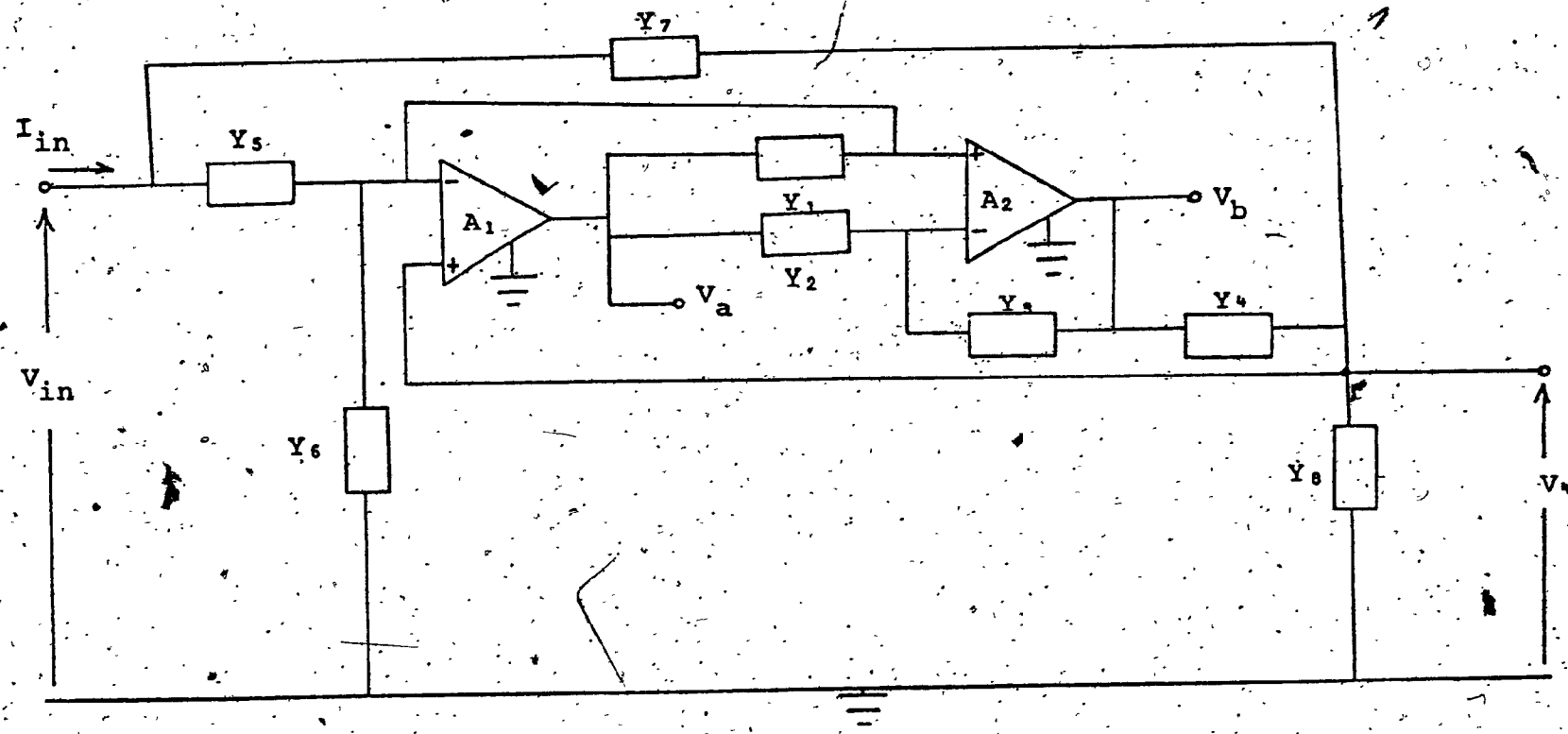

FIG. 2.2 (b) Basic Structure Incorporating Riordan's GIC

$$\begin{bmatrix} I_{in} \\ 0 \\ 0 \\ 0 \end{bmatrix} = \begin{bmatrix} Y_5+Y_7 & -Y_5 & 0 & -Y_7 \\ -Y_5 & Y_5+Y_6+Y_1(1+A_1) & 0 & -A_1Y_1 \\ 0 & A_1Y_2 - A_2Y_3 & Y_2+Y_3(1+A_2) & -A_2Y_2 \\ -Y_7 & -A_2Y_4 & A_2Y_2 & Y_4+Y_7+Y_8 \end{bmatrix} \begin{bmatrix} V_{in} \\ V_i \\ V_3 \\ V_4 \end{bmatrix} \tag{2.8}$$

From Eq. (2.8) the open circuit voltage transfer functions can be calculated as

$$T_1(s) = \frac{V_a}{V_{in}} = \frac{A_1(V_4-V_i)}{V_{in}}$$

$$= \frac{Y_1Y_3Y_7+Y_3Y_6Y_7+Y_2Y_4Y_5-Y_3Y_5Y_8-\frac{1}{A_2}(Y_2Y_6Y_7-Y_2Y_4Y_5-Y_2Y_5Y_8)}{D(s)} \tag{2.9a}$$

$$T_2(s) = \frac{V_b}{V_{in}} = \frac{A_2(V_i-V_3)}{V_{in}}$$

$$= \frac{Y_2Y_4Y_5+Y_2Y_5Y_8+Y_1Y_3Y_7-Y_2Y_6Y_7-\frac{1}{A_1}(Y_2Y_4Y_5+Y_2Y_5Y_7+Y_2Y_5Y_8)}{D(s)} \tag{2.9b}$$

$$T_3(s) = \frac{V_4}{V_{in}} = \{Y_2Y_4Y_5+Y_1Y_3Y_7+\frac{Y_1Y_7}{A_2}(Y_2+Y_3) + \frac{Y_3Y_7}{A_1}(Y_1+Y_5+Y_6)$$

$$+ \frac{Y_4Y_5}{A_1}(Y_2+Y_3) + \frac{Y_2Y_7}{A_1A_2}(Y_5+Y_6)\}/D(s) \tag{2.9c}$$

where

$$D(s) = (Y_5+Y_6)\{Y_2Y_4+(Y_4+Y_7+Y_8)(\frac{Y_2+Y_3}{A_1A_2}+\frac{Y_3}{A_1})\}$$

$$+ (Y_4+Y_7+Y_8)(\frac{Y_1Y_2}{A_1A_2}+\frac{Y_1Y_2}{A_2})$$

$$+ Y_1Y_3\{(Y_4+Y_7+Y_8)(\frac{1}{A_1}+\frac{1}{A_2}+\frac{1}{A_1A_2})+Y_7+Y_8\} \quad (2.9d)$$

If it is assumed that the Op.Amps. are ideal the voltage transfer functions become

$$T_1(s) = \frac{Y_1Y_3Y_7+Y_3Y_6Y_7+Y_2Y_4Y_5-Y_3Y_5Y_8}{(Y_5+Y_6)Y_2Y_4 + (Y_7+Y_8)Y_1Y_3}$$

$$= \frac{Y_5 + h(s)\{Y_7+Y_6Y_7/Y_1-Y_5Y_8/Y_1\}}{Y_5+Y_6 + h(s)\{Y_7+Y_8\}} \quad (2.10a)$$

$$T_2(s) = \frac{Y_2Y_4Y_5+Y_2Y_5Y_8+Y_1Y_3Y_7-Y_2Y_6Y_7}{(Y_5+Y_6)Y_2Y_4 + (Y_7+Y_8)Y_1Y_3}$$

$$= \frac{Y_8+Y_5Y_8/Y_4+h(s)Y_7-Y_6Y_7/Y_4}{Y_5+Y_6 + h(s)\{Y_7+Y_8\}} \quad (2.10b)$$

$$T_3(s) = \frac{Y_5 + h(s)Y_7}{Y_5+Y_6 + h(s)\{Y_7+Y_8\}} \quad (2.10c)$$

where

$$h(s) = Y_1Y_3/Y_2Y_4$$

as was shown earlier.

2.3.2 Element Identification for Commonly Used Biquads

Very often Butterworth, Chebychev, Bessel or elliptic approximations are used in filter design. Thus the trans-

mission zeros are located either at the origin, imaginary axis or infinity except in the case of an all - pass. Thus the transfer function given in Eq. (1.1) can be expressed as a product of biquadratic transfer functions such as

$$T_j(s) = \frac{a_{j_2}s^2 + a_{j_1}s + a_{j_0}}{b_{j_2}s^2 + b_{j_1}s + b_{j_0}} \qquad (2.11)$$

where

$a_{j_2} = a_{j_1} = 0$ for low pass (LP)

$a_{j_1} = a_{j_0} = 0$ for high pass (HP)

$a_{j_2} = a_{j_0} = 0$ for band pass (BP)

$a_{j_1} = 0$ for notch (N)

and $a_{j_2} = b_{j_2}, a_{j_1} = -b_{j_1}, a_{j_0} = b_{j_0}$ for all pass (AP) sections.

The transfer function $T_j(s)$ is characterized by Q_j and ω_{0_j} defined in Eqs. (1.10a) and (1.10b) respectively. For notch and all pass sections $T_j(s)$ is further characterized by:

Notch (N): $\omega_{nj} = (a_{j_0}/a_{j_2})^{\frac{1}{2}}$ (2.12a)

All pass (AP): $\omega_{zj} = (a_{j_0}/a_{j_2})^{\frac{1}{2}}$ (2.12b)

$Q_{zj} = (a_{j_0}a_{j_2})^{\frac{1}{2}}/a_{j_1}$. (2.12c)

By comparing Eq. (2.10) with Eq. (2.11) it becomes easy to envisage the selection of $Y_1 \ldots Y_8$ that will ensure that Eq. (2.11) is always obtained for the different a_j's

and b_j's. Table 2.1 gives one possible set of selections for LP,HP,BP,N and AP sections.

With the exception of the notch section, the output ports of all sections are obtained at the output terminals of an Op.Amp. It is possible to obtain notch sections at the output of an Op.Amp. but then, one must use iterative and/or capacitive tuning for post design adjustments of the section.

2.4 STABILITY ANALYSIS

It has been shown [10] that some networks design with Riordan's GIC can become unstable when a circuit locks in an unstable mode as a result of transient values of Op. Amp. gains following activation. Here, the stability properties of the basic configuration shown in Figure (2.2b) are examined.

It was shown earlier that the transfer functions

$$\frac{V_K}{V_{in}} = \frac{N_K(s)}{D(s)}$$

where $K = a,b,4$ and

$$D(s) = (Y_5+Y_6)\{Y_2Y_4+(Y_4+Y_7+Y_8)(\frac{Y_2+Y_3}{A_1A_2}+\frac{Y_3}{A_1})\}$$
$$+(Y_4+Y_7+Y_8)(\frac{Y_1Y_2}{A_1A_2}+\frac{Y_1Y_2}{A_2})$$
$$+Y_1Y_3\{(Y_4+Y_7+Y_8)(\frac{1}{A_1}+\frac{1}{A_2}+\frac{1}{A_1A_2})+Y_7+Y_8\} \qquad (2.9d)$$

TABLE 2.1 ELEMENT IDENTIFICATION

Circuit	Y_1	Y_2	Y_3	Y_4	Y_5	Y_6	Y_7	Y_8	Transfer Function	Remarks
1	sC_1	G_2	sC_3+G_3	G_4	G_5	0	0	G_8	$T_2(s) = \frac{G_2G_5(G_4+G_8)}{S^2C_1C_3G_8+sC_1G_3G_8+G_2G_4G_5}$	LP
2	G_1	G_2	sC_3	G_4	0	G_6	sC_7	G_8	$T_1(s) = \frac{S^2C_3C_7(G_1+G_6)}{S^2C_3C_7G_1+sC_3G_1G_8+G_2G_4G_6}$	HP
3	G_1	G_2	sC_3	G_4	0	G_6	G_7	sC_8	$T_1(s) = \frac{SC_3G_7(G_1+G_6)}{S^2C_3C_8G_1+sC_2G_1G_7+G_2G_4G_6}$	BP
4	G_1	G_2	sC_3	G_4	G_5	G_6	sC_7	sC_8+G_8	$T_3(s) = \frac{S^2C_3C_7G_1+G_2G_4G_5}{S^2C_3(C_7+C_8)G_1+sC_3G_1G_8+G_2G_4(G_5+G_6)}$	N
5	G_1	G_2	sC_3	G_4	G_5	0	sC_7	G_8	$T_1(s) = \frac{S^2C_3C_7G_8-SC_3G_5G_8+G_2G_4G_5}{S^2C_3C_7G_1+sC_3G_1G_8+G_2G_4G_5}$	AP if $G_1 = G_5$

The natural frequencies of the network in Figure (2.2b) are the zero's of the characteristic polynomial D(s) given by Eq.(2.9b).

The Op.Amp. gains can assume values in the range

$$0 \leq A_1, A_2 \leq |A_{max}| < \infty \qquad (2.13)$$

It was pointed out earlier that for a compensated Op.Amp.

$$A(s) = \frac{A_0 \omega_c}{s + \omega_c} \qquad (1.6)$$

Here we will examine the region where $|s| << \omega_c$. Thus A_1 and A_2 can be assumed to be real. The region where $|s| > \omega_c$ is studied in Chapter III. For real A_1 and A_2 and any choice of element values to produce second-order transfer functions the coefficients of D(s) are seen to remain positive for all attainable values of A_1 and A_2 owing to the absence of negative terms in D(s). A consequence of this observation is that the roots of D(s) will remain in the left-half s-plane and low frequency unstable modes cannot arise during activation.

2.5 SENSITIVITY ANALYSIS

The Q_p and ω_p sensitivities for the circuits given in Table 2.4 are analysed here with the objective of choosing the passive element values so that these sensitivities are minimized.

For future reference, some definitions and assumptions are introduced here. The sensitivity of a function F with respect to an element X is defined as

$$S_X^F = \frac{X}{F}\frac{\partial F}{\partial x} \qquad (2.14)$$

Consider a polynomial of a second order of the form

$$D(s) = b_2 s^2 + b_1 s + b_0 \qquad (2.15a)$$

$$= b_2 (s^2 + \frac{\omega_0}{Q_p} + \omega^2) \qquad (2.15b)$$

where

$$\frac{b_1}{b_2} = \frac{\omega_0}{Q_p} \qquad (2.15c)$$

and

$$\frac{b_0}{b_2} = \omega_0^2 \qquad (2.15d)$$

Assuming that each of these expressions is a function of x, the following expressions can easily be derived for the Q_p- and ω_0- sensitivities.

$$S_x^{\omega_0} = \tfrac{1}{2}(S_x^{b_0} - S_x^{b_2}) \qquad (2.16)$$

$$S_x^{Q_p} = \tfrac{1}{2}(S_x^{b_0} + S_x^{b_2}) - S_x^{b_1} \qquad (2.17)$$

For the Op.Amps. a single-pole response of the form of Eq. (1.6) is assumed for the gains A_1 and A_2. It is further assumed that $A_1 = A_2 = A$. This is a reasonable assumption

to make since it would be more practical to build the circuits under consideration with dual IC Op.Amps. Measurements made on dual IC Op.Amps. [16] have shown very good tracking of A_1 and A_2 over a wide temperature range.

Thus,

$$A_1 = A_2 = A = \frac{A_0 \omega_c}{s + \omega_c} = \frac{B}{s + \omega_c} \qquad (2.18a)$$

and

$$\frac{1}{A} = \frac{1}{A_0} + \frac{s}{B} \qquad (2.18b)$$

Low frequency operation is considered here so that it can reasonably be stated that

$$\frac{1}{A} \simeq \frac{1}{A_0} \qquad (2.19)$$

For presently available Op.Amps. $\frac{1}{A_0} >> \frac{1}{A_0^2}$ so that all terms containing $\frac{1}{A_0^2}$ will be neglected.

With the above assumptions the denominator polynomial D(s) given in Eq. (2.9d) reduces to

$$D(s) \simeq (Y_5+Y_6)\{Y_2Y_4 + \frac{Y_3}{A_0}(Y_4+Y_7+Y_8)\}$$
$$+ \frac{Y_1Y_2}{A_0}(Y_4+Y_7+Y_8)$$
$$+ Y_1Y_3\{Y_7+Y_8+\frac{2}{A_0}(Y_4+Y_7+Y_8)\} \qquad (2.20)$$

2.5.1 Passive ω_0-and Q_p-Sensitivities

For ideal Op.Amps. (i.e. $\frac{1}{A_0} \to 0$) and by using Table 2.1, (Eq.2.14-2.17) and (Eq.2.20), it is a straightforward matter to show that

$$\left|S^{Q_p}_{R,C}\right| < 1 \text{ and } \left|S^{\omega_0}_{R,C}\right| < 1 \qquad (2.21)$$

2.5.2 Active ω_0-and Q_p-Sensitivities

2.5.2.1 Circuit 1 (from Table 2.1)

The passive elements of this LP section are identified as

$$Y_1 = sC_1,\ Y_2 = G_2,\ Y_3 = sC_3 + G_3,\ Y_4 = G_4$$

$$Y_5 = G_5,\ Y_6 = 0,\ Y_7 = 0,\ Y_8 = G_8$$

Substitution of these values in Eq. (2.20) yields

$$D(s) = S^2[C_1C_3G_8 + \frac{2}{A_0}C_1C_3(G_4 + G_8)]$$

$$+ S\,[C_1G_3G_8 + \frac{G_4+G_8}{A_0}(2C_1G_3 + C_1G_2 + C_3G_5)]$$

$$+ [G_2G_4G_5 + \frac{G_3G_5}{A_0}(G_4 + G_8)] \qquad (2.22)$$

From Eq. (2.22) the ideal ($\frac{1}{A_0} \to 0$) Q_p and ω_0 are given by

$$Q_p^2 = (G_2G_4G_5C_3)/(G_3^2G_8C_1) \qquad (2.23a)$$

$$\omega_0^2 = (G_2 G_4 G_5)/(C_1 C_3 G_8) \qquad (2.23b)$$

On application of Eqs. (2.14) - (2.17) to Eq.(2.22) one obtains

$$S_{A_0}^{b_2} = -\frac{2}{A_0^2} C_1 C_3 (G_4+G_8) \cdot \frac{A_0^2}{A_0 C_1 C_3 G_8 + 2C_1 C_3 (G_4+G_8)}$$

$$\simeq -\frac{2(G_4+G_8)}{A_0 G_8} \qquad (2.24a)$$

$$S_{A_0}^{b_1} \simeq -\frac{(G_4+G_8)(G_2+2G_3)}{A_0 G_3 G_8} - \frac{(G_4+G_8)(C_3 G_5)}{A_0 G_3 G_8 C_1} \qquad (2.24b)$$

and $$S_{A_0}^{b_0} \simeq \frac{G_3(G_4+G_8)}{A_0 G_2 G_4} \qquad (2.24c)$$

From above

$$S_{A_0}^{\omega_{oa}} \simeq \frac{1}{2A_0}\left[\frac{2(G_4+G_8)}{G_8} - \frac{G_3(G_4+G_8)}{G_2 G_4}\right] \qquad (2.25a)$$

and

$$S_{A_0}^{Q_{pa}} \simeq \frac{1}{2A_0}\left[\frac{2(G_4+G_8)(G_2+2G_3)}{G_3 G_8} + \frac{2(G_4+G_8)G_5 C_3}{G_3 G_8 C_1} - \right.$$

$$\left. - \frac{G_3(G_4+G_8)}{G_2 G_4} - \frac{2(G_4+G_8)}{G_8}\right] \qquad (2.25b)$$

where Q_{pa} and ω_{oa} are the non-ideal pole-Q and pole frequency calculable from Eq. (2.22).

Define

$$X = \frac{G_3}{G_2} \tag{2.26a}$$

and

$$Z = \frac{G_8}{G_4} \tag{2.26b}$$

Using Eq.(2.26) and Eqs.(2.23a),(2.25b) becomes

$$S_{A_0}^{Q_{pa}} = \frac{1}{2A_0}\left[\frac{2}{XZ} + \frac{2}{Z} + \frac{2}{X} + 2Q_p^2X + 2Q_p^2XZ + \right.$$

$$\left. + 2 - X - XZ\right] \tag{2.27}$$

If it is assumed that the negative terms in Eq. (2.27) are negligible in comparison to the positive terms (the consequence of this assumption is examined below), then Eq.(2.27) reduces to

$$S_{A_0}^{Q_{pa}} = \frac{1}{2A_0}\left[\frac{2}{XZ} + \frac{2}{Z} + \frac{2}{X} + 2Q_p^2X + 2Q^2XZ + 2\right] \tag{2.28}$$

At this point our intention is to minimize $S_{A_0}^{Q_{pa}}$. Attempts to minimize Eq. (2.28) using differential calculus results in non-linear simultaneous equations which are rather tedious to solve. Pattern search techniques will be used. The form of Eq. (2.28) shows that $S_{A_0}^{Q_{pa}}$ would be minimized for $Z = K$ and $X = \alpha/Q_p$ where K and α are constants.

Letting $Z = 1$, Eq. (2.28) becomes

$$S_{A_0}^{Q_{pa}} = \frac{1}{2A}\left[\frac{4}{X} + 4Q_p^2X + 4\right] \tag{2.29}$$

and it is obvious that Eq. (2.29) is minimized for $X = \frac{1}{Q_p}$. Now, let $X = \frac{1}{Q_p}$ in Eq. (2.28) and search on Z, i.e.,

$$S_{A_0}^{Q_{pa}} = \frac{1}{2A_0}\left[\frac{2Q_p}{Z} + \frac{2}{Z} + 4Q_p + 2Q_pZ + 2\right] \qquad (2.30)$$

Thus $S_{A_0}^{Q_{pa}}$ is minimized for

$$\frac{dS_{A_0}^{Q_{pa}}}{dZ} = \frac{1}{2A_0}\left[-\frac{2Q_p}{Z^2} - \frac{2}{Z^2} + 2Q_p\right] = 0 \qquad (2.31a)$$

or $$Z = \sqrt{1 + 1/Q_p} \simeq 1 \text{ for } (Q \gg 1) \qquad (2.31b)$$

Thus we can conclude that the minimum value of value of $S_{A_0}^{Q_{pa}}$ is found at

$$Z = \frac{G_6}{G_4} = 1 \qquad (2.32a)$$

and

$$X = \frac{G_3}{G_2} = \frac{1}{Q_p} \qquad (2.32b)$$

Substituting for $Z = 1$ and $X = \frac{1}{Q_p}$ in Eq. (2.25a) and Eq. (2.28) we obtain

$$S_{A_0}^{\omega_{oa}} = \frac{2}{A_0} - \frac{1}{A_0Q_p} \simeq \frac{2}{A_0} \qquad (2.33a)$$

and

$$S_{A_0}^{Q_{pa}} = \frac{1}{2A_0}\left[8Q_p + 4\right] \simeq \frac{4Q_p}{A_0} \qquad (2.33b)$$

In arriving at the above results, it was necessary to assume that the negative terms in Eq. (2.27) were negligible in comparison to the positive terms. With the above

values for Z and X this assumption is valid provided

$$2Q_p + 2 + 2Q_p + 2Q_p + 2Q_p + 2 >> \frac{2}{Q_p}$$

i.e.

$$8Q_p + 4 \gtrsim \frac{2}{Q_p} \qquad (2.34)$$

2.5.2.2 Circuits 2,3,4,5 (from Table 2.1)

The passive elements of these circuits can be identified as

$$Y_1 = G_1, Y_2 = G_2, Y_3 = sC_3, Y_4 = G_4, Y_5 = G_5,$$
$$Y_6 = G_6, Y_7 = sC_7 + G_7 \text{ and } Y_8 = sC_8 + G_8$$

With the values the denominator polynomial Eq. (2.20) is

$$D(s) \simeq S^2[C_3(C_7+C_8)G_1+\frac{C_3}{A_0}(C_7+C_8)(2G_1+G_5+G_6)]$$
$$+ S[G_1(G_7+G_8)C_3+\frac{C_3}{A_0}(G_4+G_7+G_8)(2G_1+G_5+G_6)$$
$$+ \frac{G_1G_2}{A_0}(C_7+C_8)] + [G_2G_4(G_5+G_6) + \frac{G_1G_2}{A_0}(G_4$$
$$+ G_7+G_8)] \qquad (2.35)$$

As $A_0 \to \infty$ one obtains

$$Q_p^2 = \frac{G_2G_4(G_5+G_6)(C_7+C_8)}{G_1(G_7+G_8)^2C_3} \qquad (2.36a)$$

and

$$\omega_0^2 = \frac{G_2G_4(G_5+G_6)}{G_1C_3(C_7+C_8)} \qquad (2.36b)$$

For finite values of A_0 we again derive

$$S_{A_0}^{\omega_{oa}} \simeq \frac{1}{2A_0}\left[\frac{2G_1+G_5+G_6}{G_1} - \frac{G_1(G_4+G_7+G_8)}{G_4(G_5+G_6)}\right] \qquad (2.37a)$$

and

$$S_{A_0}^{Q_{pa}} = \frac{1}{2A_0}\left[\frac{2(G_4+G_7+G_8)(2G_1+G_5+G_6)}{G_1(G_7+G_8)}\right.$$

$$\left. + \frac{2G_2(C_7+C_8)}{C_3(G_7+G_8)} - \frac{2G_1+G_5+G_6}{G_1} - \frac{G_1(G_4+G_7+G_8)}{G_4(G_5+G_6)}\right] \qquad (2.37b)$$

Let

$$m = \frac{(G_7+G_8)}{G_4} \qquad (2.38a)$$

$$n = \frac{(G_5+G_6)}{G_1} \qquad (2.38b)$$

Substituting in Eq.(2.37b) one obtains

$$S_{A_0}^{Q_{pa}} = \frac{1}{2A_0}\left[\frac{4}{m} + \frac{2n}{m} + n + 2Q_p^2\frac{m}{n} + 2 - \frac{m}{n} - \frac{1}{n}\right] \qquad (2.39)$$

Using search techniques it is found that $S_{A_0}^{Q_{pa}}$ is minimized for

$$m = \frac{2}{Q_p} \qquad (2.40a)$$

and

$$n = 2 \qquad (2.40b)$$

provided

$$6Q_p + 4 >> \frac{1}{2} + \frac{1}{Q_p} \qquad (2.41)$$

The corresponding values for $S_{A_0}^{\omega_{oa}}$ and $S_{A_0}^{Q_{pa}}$ are

$$S_{A_0}^{\omega_{oa}} \simeq \frac{7}{4A_0} \qquad (2.42a)$$

$$S_{A_0}^{Q_{pa}} \simeq \frac{3Q_p}{A_0} \qquad (2.42b)$$

2.6 DESIGN PROCEDURE

2.6.1 Design A

An inspection of Table 2.1 and the defining expressions for Q_p and ω_0 shows that element values can be selected in several ways. The degree of freedom in selecting element values can be used to obtain an acceptable spread in element values and/or minimize the active sensitivity $S_{A_0}^{Q_{pa}}$. A design using the low $S_{A_0}^{Q_{pa}}$ sensitivity constraints of Eq. (2.32) and Eq.(2.40) is given here. Equal capacitance design is obtained and the maximum spread in resistance values is Q_p. Circuits 2,3,4 and 5 require three different values of resistors. This might be an inventory problem if discrete components are used to construct these circuits. An all pass section cannot be obtained from Circuit 5 if the $S_{A_0}^{Q_{pa}}$ are used since, a priori, G_1 must be equal to G_5 to achieve all pass sections. Using Table 2.1 and the defining relations for ω_n, ω_0 and Q_p it is seen that these parameters can be adjusted by trimming three distinct resistors. The tuning sequence is given alongside with the design in Table 2.2.

TABLE 2.2 DESIGN VALUES AND TUNING SEQUENCE - DESIGN A

Circuit Number	Design Values	Transfer Function Realized	Tuning Sequence ω_n	Tuning Sequence ω_o	Tuning Sequence Q_p
1	Choose $C_1 = C_3 = G/\omega_o$ $G_2 = G_4 = G_5 = G_6 = G$, $G_3 = G/Q_p$	$T_2(s) = \frac{2\omega_o^2}{D(s)}$	-	G_6	G_3
2	Choose $C_3 = C_7 = G/\omega_o$ $G_2 = G_6 = G$, $G_1 = G_4 = G/2$, $G_8 = G/Q_p$	$T_1(s) = \frac{3s^2}{D(s)}$	-	G_4	G_8
3	Choose $C_3 = C_8 = G/\omega_o$ $G_2 = G_6 = G$, $G_1 = G_4 = G/2$, $G_7 = G/Q_p$	$T_1(s) = \frac{3(\omega_o/Q_p)s}{D(s)}$	-	G_1	G_7
4	Choose $C_3 = C_7 + C_8 = G/\omega_o$ $G_2 = G_5 + G_6 = G$, $G_1 = G_4 = G/2$, $G_8 = G/Q_p$ $\omega_n^2 = \omega_o G_5/C_7$	$T_3(s) = \frac{C_7}{C_7 + C_8} \cdot \frac{s^2 + \omega_n^2}{D(s)}$	G_1	G_6	G_8
5	Not possible with sensitivity constraints				

$$D(s) = S^2 + \frac{\omega_o}{Q_p}s + \omega_o^2$$

2.6.2 Design B

It is noted that in design A circuits 2,3,4 need three different resistant values. This is a consequence of the minimum sensitivity constraints imposed on $S_{A_0}^{Q_{pa}}$.

Moreover, the all pass section of Circuit 5 cannot be designed using the minimum sensitivity constraints. However, the sensitivity $S_{A_0}^{Q_{pa}}$ varies very slowly with respect to m and n.

If m and n are chosen as

$$m = \frac{1}{Q_p} \tag{2.43a}$$

$$n = 1$$

we find from Eq. (2.39) that

$$S_{A_0}^{Q_{pa}} \simeq \frac{4Q_p}{A_0} \tag{2.44a}$$

and from Eq. (2.37a) that

$$S_{A_0}^{\omega_{oa}} \simeq \frac{1}{A_0} \tag{2.44b}$$

Conditions (2.43a) and (2.43b) are used in Design B. The resulting design values are shown in Table 2.3.

TABLE 2.3 DESIGN VALUES AND TUNING SEQUENCE - DESIGN B

Circuit Number	Design Values	Transfer Function Realized	Tuning Sequence		
			ω_n	ω_0	Q_p
1	Choose $C_1 = C_3 = G/\omega_0$ $G_2 = G_4 = G_5 = G_8 = G$, $G_3 = G/Q_p$	$T_2(s) = \frac{2\omega_0^2}{D(s)}$	-	G_8	G_3
2	$C_3 = C_7 = G/\omega_0$ $G_1 = G_2 = G_4 = G_6 = G$, $G_8 = G/Q_p$	$T_1(s) = \frac{2s^2}{D(s)}$	-	G_4	G_8
3	$C_3 = C_8 = G/\omega_0$ $G_1 = G_2 = G_4 = G_6 = G$, $G_7 = G/Q_p$	$T_1(s) = \frac{2(\omega_0/Q_p)s}{D(s)}$	-	G_1	G_7
4	$C_3 = C_7 + C_8 = G/\omega_0$ $G_1 = G_2 = G_4 = G_5 = G_6 = G$ $\omega_n^2 = \omega_0 G_5/C_7$	$T_3(s) = \frac{C_7}{C_7 + C_8} \cdot \frac{s^2 + \omega_n^2}{D(s)}$	G_1	G_6	G_8
5	$C_3 = C_4 = G/\omega_0$ $G_1 = G_2 = G_4 = G_5 = G$, $G_8 = G/Q_p$	$T_1(s) = \frac{D(-s)}{D(s)}$	G_4	G_6	G_3

$$D(s) = s^2 + \frac{\omega_0}{Q_p}s + \omega_0^2$$

2.7 CONCLUSIONS

A configuration incorporating Riordan's GIC has been used to derive a number of universal second-order RC-active sections. Each of these sections contains two Op.Amps. The sensitivities of Q_p and ω_0 of these networks with respect to the passive and active element variations are found to be low. In addition, these sections are free from low frequency unstable modes of operation.

With the exception of the notch section, the output ports of all the sections are obtained at the output terminals of an Op.Amp. Thus the output impedance of these sections is very low. Tuning for the desired ω_0 and Q_p in these networks is easily accomplished. A tuning sequence using only resistors has been described for the derived sections. These sections are shown explitly in Figure 2.3.

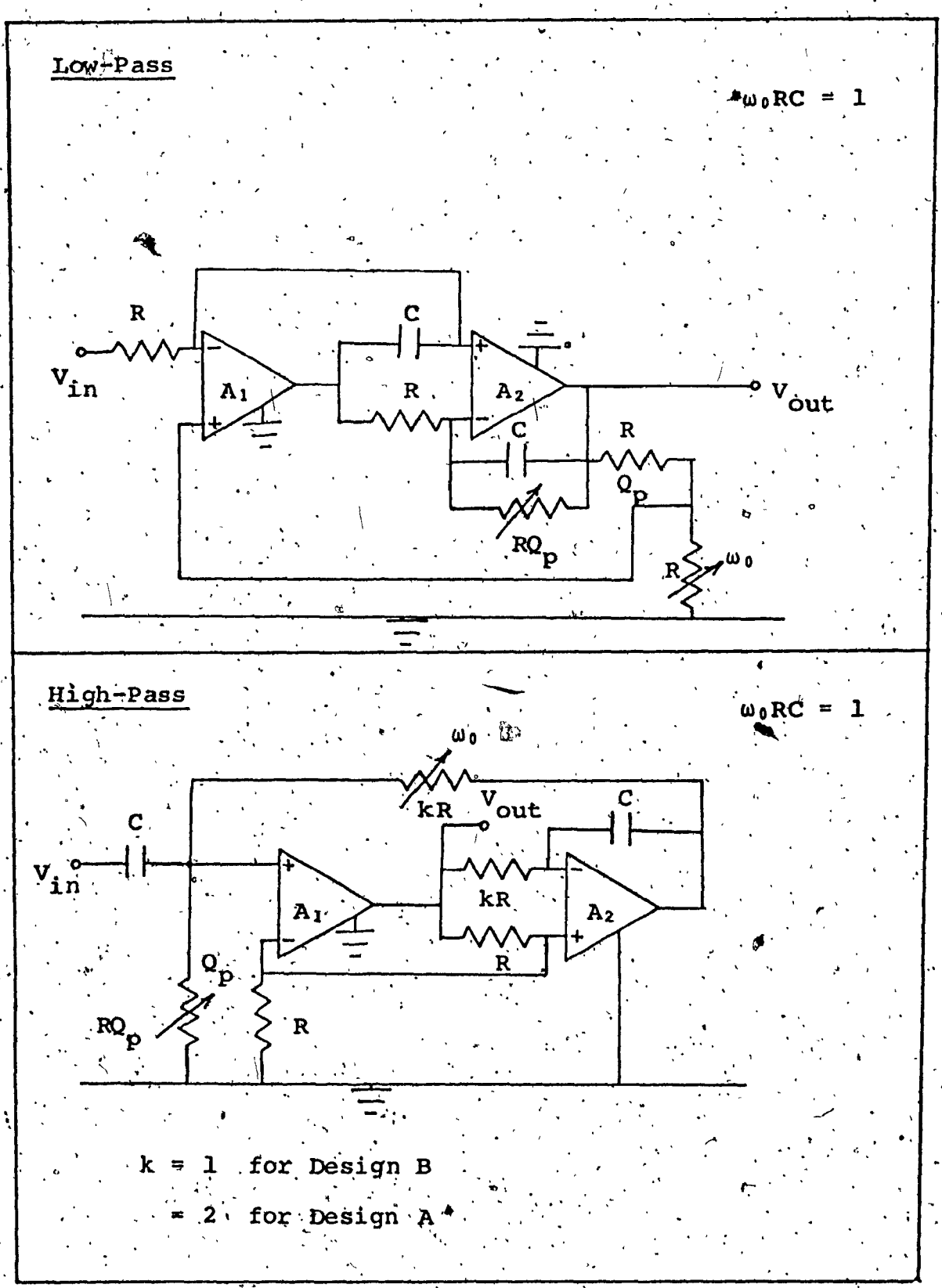

FIG. 2.3 Resulting Second-Order Filter Sections

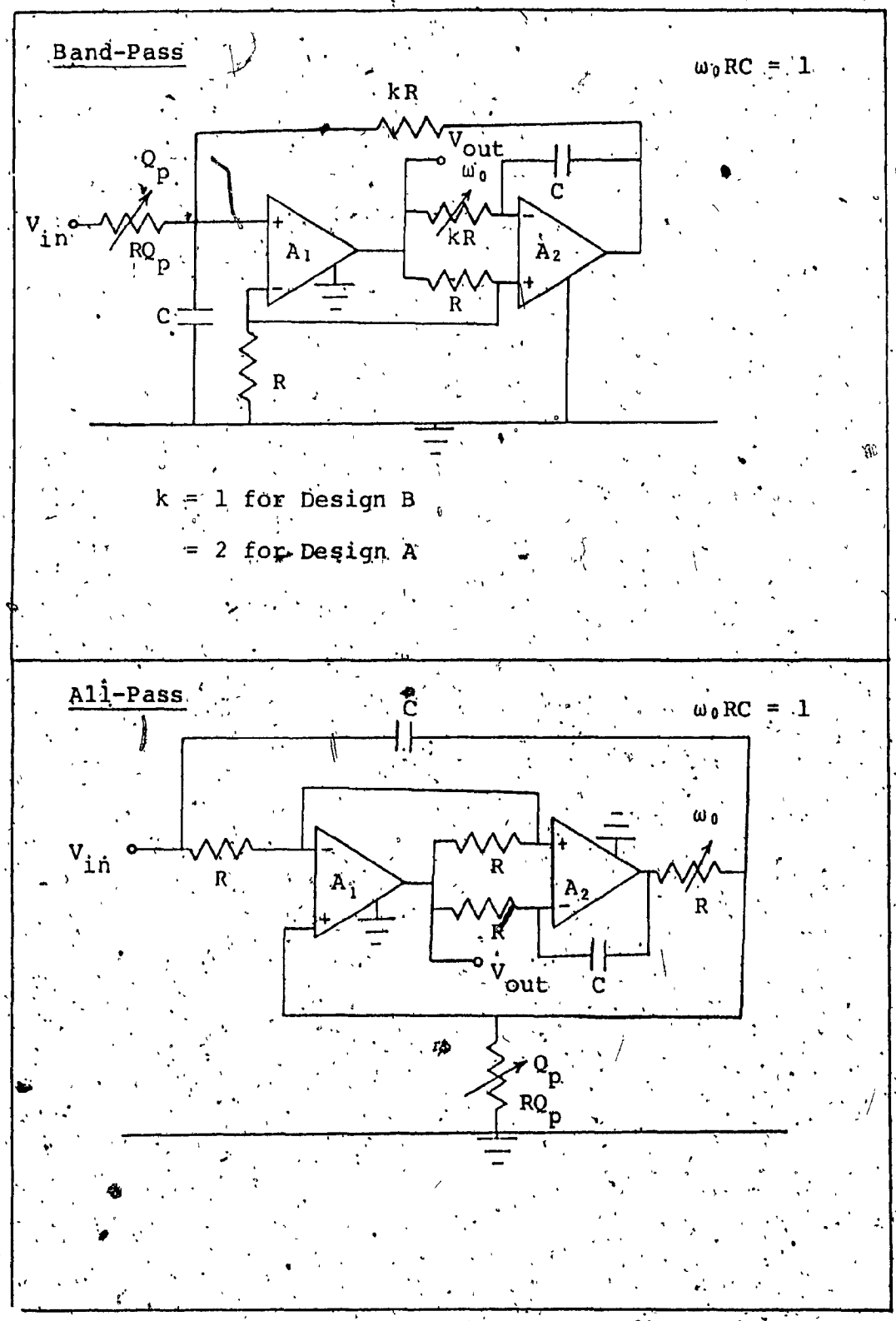

FIG. 2.3 (continued).

Notch

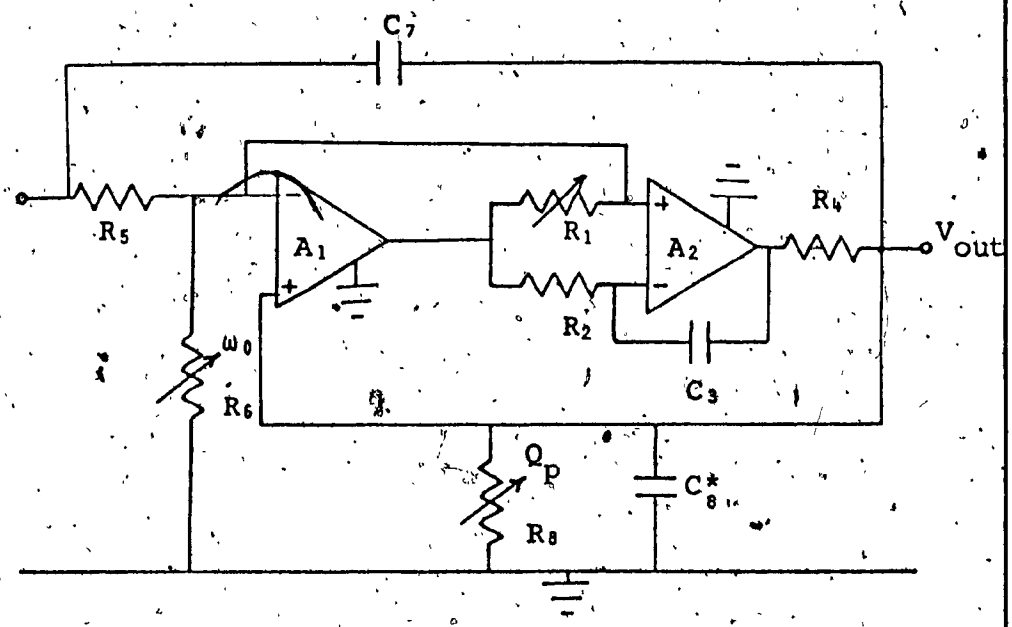

For Design A - See Table 2.2, Circuit No. 4

For Design B - See Table 2.3, Circuit No. 4

* Not necessary if $\omega_n < \omega_0$

FIGURE 2.3 (continued)

CHAPTER III

EFFECT OF OP AMP IMPERFECTIONS ON DERIVED BIQUADS

3.1 INTRODUCTION

It was pointed out earlier that the commercially available Op.Amp. may differ significantly from the idealized Op.Amp. The imperfections of the practical Op.Amp. tend to have an adverse effect on filter performance. In Chapter II, it was shown how the effect of finite dc gain, A_0, of the Op. Amp. can be reduced. In this Chapter, the effect of some of the imperfections of the Op. Amp. on filter performance is estimated.

3.2 Q_p AND ω_0 DEPENDENCE ON A_0

In the region where $|S| < \omega_c$, the finite value of A_0 becomes the dominant active perameter that may deteriorate filter performance. Here we derive the Q_p and ω_0 dependence on A_0 for the circuits designed in Chapter II.

3.2.1 Circuit No. 1

The denominator polynomial for Circuit 1 is given from Eq. (2.22) as

$$D(s) \simeq S^2[C_1C_3G_8 + \frac{2}{A_0}C_1C_3(G_4+G_8)]$$

$$+ S[C_1G_3G_8 + \frac{G_4+G_8}{A_0}(2C_1G_3 + C_1G_2 + C_3G_5)]$$

$$+ [G_2G_4G_5 + \frac{G_3G_5}{A_0}(G_4+G_8)] \qquad (2.22)$$

From Eq. (2.22) we calculate

$$Q_{pa}^2 = \frac{[C_1C_3G_8 + \frac{2}{A_0}C_1C_3(G_4+G_8)][G_2G_4G_5 + \frac{G_3G_5}{A_0}(G_4+G_8)]}{[C_1G_3G_8 + \frac{G_4+G_8}{A_0}(2C_1G_3 + C_1G_2 + C_3G_5)]^2} \qquad (3.1a)$$

$$= \frac{Q_p^2[1 + \frac{2(G_4+G_8)}{A_0G_8}][1 + \frac{G_3}{A_0G_2}\frac{G_4+G_8}{G_4}]}{[1 + \frac{G_4+G_8}{A_0G_8}][1 + \frac{G_3}{A_0G_2}\frac{G_4+G_8}{G_4}]} \qquad (3.1b)$$

where Q_p is given by Eq. (2.23).

By substituting the design values for Design A and Design B (Tables 2.2 and 2.3), Eq.(3.1) reduces to

$$Q_{pa}^2 = \frac{Q_p^2[1 + \frac{4}{A_0}][1 + \frac{2}{A_0Q_p}]}{[1 + \frac{2}{A_0}(2 + 2Q_p)]^2} \qquad (3.2a)$$

$$= \frac{Q_p^2[1 + \frac{2}{A_0Q_p} + \frac{4}{A_0} + \frac{8}{A_0^2Q_p}]}{[1 + \frac{4}{A_0} + \frac{4Q_p}{A_0}]^2} \qquad (3.2b)$$

and

$$Q_{pa} \simeq \frac{Q_p}{1 + \frac{4Q_p}{A_0}} \qquad (3.2c)$$

In a similar manner, ω_{0a} can be shown to be given by

$$\omega_{0a} = \frac{\omega_0}{1 + \frac{2}{A_0}} \tag{3.3}$$

3.2.2 Circuits Nos. 2,3,4,5

For these circuits, the denominator polynomial is given by Eq. (2.35).

$$\begin{aligned} D(s) = {} & s^2[C_3(C_7+C_8)G_1 + \frac{C_3}{A_0}(C_7+C_8)(2G_1+G_5+G_6)] \\ & + s[G_1(G_7+G_8)C_3 + \frac{C_3}{A_0}(G_4+G_7+G_8)(2G_1+G_5+G_6) \\ & + \frac{G_1G_2}{A_0}(C_7+C_8)] + [G_2G_4(G_5+G_6) \\ & + \frac{G_1G_2}{A_0}(G_4+G_7+G_8)] \end{aligned} \tag{2.35}$$

From Eq. (2.35) Q_{pa} is found to be given by

$$Q_{pa}^2 = \frac{[C_3(C_7+C_8)G_1 + \frac{C_3}{A_0}(C_7+C_8)(2G_1+G_5+G_6)][G_2G_4(G_5+G_6) + \frac{G_1G_2}{A_0}(C_7+C_8)]}{[G_1(G_7+G_8)C_3 + \frac{C_3}{A_0}(G_4+G_7+G_8)(2G_1+G_5+G_6) + \frac{G_1G_2}{A_0}(C_7+C_8)]^2} \tag{3.4a}$$

$$= \frac{Q_p^2[1 + \frac{2G_1+G_5+G_6}{A_0G_1}][1 + \frac{G_1}{(G_5+G_6)A_0} \cdot \frac{G_4+G_7+G_8}{G_4}]}{[1 + \frac{1}{A_0}\frac{G_4+G_7+G_8}{G_7+G_8} \cdot \frac{2G_1+G_5+G_6}{G_1} + \frac{C_7+C_8}{A_0C_3} \cdot \frac{G_2}{G_7+G_8}]^2} \tag{3.4b}$$

For Design A, Eq. (3.4) becomes

$$Q_{pa}^2 = \frac{[1 + \frac{9}{2A_0} + \frac{2}{A_0^2} + \frac{1}{A_0 Q_p} + \frac{4}{A_0^2 Q_p}]}{[1 + \frac{4}{A_0} + \frac{3Q_p}{A_0}]^2} \qquad (3.5a)$$

and

$$Q_{pa} \approx \frac{Q_p}{1 + \frac{3Q_p}{A_0}} \qquad (3.5b)$$

For Design B, Eq. (3.4) reduces to

$$Q_{pa}^2 = \frac{Q_p^2 [1 + \frac{4}{A_0} + \frac{3}{A_0^2} + \frac{1}{A_0 Q_p} + \frac{1}{A_0^2 Q_p}]}{[1 + \frac{3}{A_0} + \frac{4Q_p}{A_0}]^2} \qquad (3.6a)$$

and

$$Q_{pa} \approx \frac{Q_p}{1 + \frac{4Q_p}{A_0}} \qquad (3.6b)$$

similarly ω_{0a} for designs A and B are given by

$$\omega_{0a} = \frac{\omega_0}{1 + \frac{7}{4A_0}} \quad \text{(Design A)} \qquad (3.7a)$$

and

$$\omega_{0a} = \frac{\omega_0}{1 + \frac{1}{A_0}} \quad \text{(Design B)} \qquad (3.7b)$$

respectively.

These results are summarized in Table 3.1.

TABLE 3.1 Q_p, ω_0 DEPENDENCE ON A_0

Design			
A	Circuit 1	$\omega_{0a} = \dfrac{\omega_0}{1 + \dfrac{2}{A_0}}$	$Q_{pa} = \dfrac{Q_p}{1 + \dfrac{4Q_p}{A_0}}$
	Circuits 2, 3 and 4	$\omega_{0a} = \dfrac{\omega_0}{1 + \dfrac{7}{4A_0}}$	$Q_{pa} = \dfrac{Q_p}{1 + \dfrac{3Q_p}{A_0}}$
B	Circuit 1	$\omega_{0a} = \dfrac{\omega_0}{1 + \dfrac{2}{A_0}}$	$Q_{pa} = \dfrac{Q_p}{1 + \dfrac{4Q_p}{A_0}}$
	Circuits 2, 3,4 and 5	$\omega_{0a} = \dfrac{\omega_0}{1 + \dfrac{1}{A_0}}$	$Q_{pa} = \dfrac{Q_p}{1 + \dfrac{4Q_p}{A_0}}$

3.3 Q_p, ω_0 DEPENDENCE ON OP.AMP.GAIN BANDWIDTH PRODUCT, B

In active filter design, the assumption of infinite bandwidth of the active element is, at best, good only for very low frequencies. Even at moderately high frequencies this assumption can lead to drastic deviations in filter performance than what is expected [17]. In this section we study the limits imposed by the finite gain bandwidth, B, of the Op. Amps. on the Q_p and ω_0 of Designs A and B.

It was shown earlier that the denominator polynomial was given by

$$D(s) = (Y_5+Y_6)\{Y_2Y_4 + (Y_4+Y_7+Y_8)(\frac{Y_2+Y_3}{A_1A_2} + \frac{Y_3}{A_1})\}$$
$$+ (Y_4+Y_7+Y_8)(\frac{Y_1Y_2}{A_1A_2} + \frac{Y_1Y_2}{A_2})$$
$$+ Y_1Y_3\{(Y_4+Y_7+Y_8)(\frac{1}{A_1} + \frac{1}{A_2} + \frac{1}{A_1A_2}) + Y_7 + Y_8\} \quad (2.9d)$$

For typical amplifiers $A_1A_2 >> A_1$ or A_2 and the second order terms (A_1A_2) in Eq. (2.9d) can be dropped. This leads to

$$D(s) \simeq (Y_5+Y_6)\{Y_2Y_4 + (Y_4+Y_7+Y_8)(\frac{Y_3}{A_1})\}$$
$$+ (Y_4+Y_7+Y_8)(\frac{Y_1Y_2}{A_2}) + Y_1Y_3\{(Y_4+Y_7+Y_8)(\frac{1}{A_1} + \frac{1}{A_2})$$
$$+ Y_7 + Y_8\} \quad (3.8)$$

For pole frequencies above 1kHz the gains for practical amplifiers can be approximated by

$$\frac{1}{A_1} = \frac{S}{B_1}$$

and

$$\frac{1}{A_2} = \frac{S}{B_2} \qquad (3.9)$$

where B_i is the gain bandwidth product of the Op.Amp.

3.3.1 Design A

Using Eq. (3.9) and the element values for Design A (Table 2.2) in Eq. (3.8), we find that

$$D'(s) = 2\omega_0^2 G^3 D(s) = S^3\left(\frac{3}{B_1} + \frac{1}{B_2}\right) + S^2\left(1 + \frac{3\omega_0}{2B_1} + \frac{3\omega_0}{2B_2} + \frac{3\omega_0}{B_1 Q_p} + \frac{\omega_0}{B_2 Q_p}\right) + S\left(\frac{\omega_0}{Q_p} + \frac{\omega_0^2}{B_2 Q_p} + \frac{\omega_0^2}{2B_2}\right) + \omega_0^2 \qquad (3.10)$$

Assuming $Q_p >> 1$, Eq. (3.10) reduces to

$$D'(s) \simeq S^3\left(\frac{3}{B_1} + \frac{1}{B_2}\right) + S^2\left(1 + \frac{3\omega_0}{2B_1} + \frac{3\omega_0}{2B_2}\right) + S\left(\frac{\omega_0}{Q_p} \quad \frac{\omega_0^2}{2B_2}\right) + \omega_0^2 \qquad (3.11)$$

The polynomial D'(s) may be written as

$$D'(s) = \left(S^2 + \frac{S\omega_{0k}}{Q_{pk}} + \omega_{0k}^2\right)\left\{\left(\frac{3}{B_1} + \frac{1}{B_2}\right)S + \frac{\omega_0^2}{\omega_{0k}^2}\right\} \qquad (3.12)$$

where ω_{0k} and Q_{pk} are the actual pole frequency and pole-Q, respectively.

By comparing coefficients of S in Eq. (3.11) and Eq. (3.12) we obtain

$$\left(\frac{3}{B_1} + \frac{1}{B_2}\right)\omega_{0k}^2 + \frac{\omega_0^2}{Q_{pk}\omega_{0k}} = \frac{\omega_0}{Q_p} + \frac{\omega_0^2}{2B_2} \qquad (3.13)$$

From Eq. (3.13) we can show that

$$\frac{Q_{pk}}{Q_p} = \frac{1}{\frac{\omega_{0k}}{\omega_0} + \frac{\omega_{0k}Q_p}{2B_2} - \frac{\omega_{0k}^3}{\omega_0^2}Q_p\left(\frac{3B_2+B_1}{B_1B_2}\right)} \qquad (3.14)$$

If we let $\omega_{0k} = \omega_0(1 + \delta)$ where $\delta << 1$ such that

$$\omega_{0k}^2 \simeq \omega_0^2(1 + 2\delta) \text{ and } \omega_{0k}^3 \simeq \omega_0^3(1 + 3\delta)$$

Eq. (3.14) reduces to

$$\frac{Q_{pk}}{Q_p} = \frac{1}{1 + \delta - \frac{7}{2B}\omega_0 Q_p - \frac{23\omega_0 Q_p \delta}{2B}} \simeq \frac{1}{1 - \frac{7}{2B}\omega_0 Q_p}$$

where it has been assumed that $B_1 \simeq B_2$.

To obtain the ω_0-deviation, the S^2-term coefficients in Eq. (3.11) and Eq. (3.12) are equated. Thus

$$\left(\frac{3}{B_1} + \frac{1}{B_2}\right)\frac{\omega_{0k}}{Q_{pk}} + \frac{\omega_0^2}{\omega_{0k}} = 1 + \frac{3\omega_0}{2B_1} + \frac{3\omega_0}{2B_2} \qquad (3.16)$$

With $\omega_{0k} = \omega_0(1 + \delta)$ and $\delta << 1$, Eq. (3.16) reduces to

$$\left(\frac{3}{B_1} + \frac{1}{B_2}\right)\left(\frac{\omega_0(1+\delta)}{Q_{pk}}\right) + \frac{1}{1+2\delta} = 1 + \frac{3\omega_0}{2B_1} + \frac{3\omega_0}{2B_2} \qquad (3.17)$$

Solving for δ we obtain

$$\delta = -\frac{\frac{3}{4}\frac{\omega_0}{B_1} + \frac{3}{4}\frac{\omega_0}{B_2} - \omega_0\left(\frac{3}{2B_1Q_{pk}} + \frac{1}{2B_2Q_{pk}}\right)}{1 + \frac{3}{2}\frac{\omega_0}{B_1} + \frac{3\omega_0}{B_2} - \frac{9}{2}\frac{\omega_0}{B_1Q_{pk}} - \frac{3}{2}\frac{\omega_0}{B_2Q_{pk}}} \qquad (3.18a)$$

$$\approx -\left(\frac{3}{4}\frac{\omega_0}{B_1} + \frac{3}{4}\frac{\omega_0}{B_2}\right) \qquad (3.18b)$$

For $B_1 = B_2$

$$\delta = -\frac{3\omega_0}{2B} \qquad (3.18c)$$

and

$$\omega_{0k} = \omega_0\left(1 - \frac{3\omega_0}{2B}\right) \qquad (3.19)$$

3.3.2 Design B.

Again when Eq. (3.9) and the element values for Design B (Table 2.3) are used in Eq. (3.8)

$$D'(s) = G^3\omega_0^2 D(s) = S^3\left(\frac{2}{B_1} + \frac{1}{B_2}\right) + S^2\left(1 + \frac{2\omega_0}{B_1} + \frac{2\omega_0}{B_1Q_p} + \frac{2\omega_0}{B_2} + \frac{\omega_0}{B_2Q_p}\right) + S\left(\frac{\omega_0}{Q_p} + \frac{\omega_0^2}{B_2} + \frac{\omega_0^2}{B_2Q_p}\right) + \omega_0^2 \qquad (3.20a)$$

For $Q_p >> 1$

$$D'(s) \simeq S^3\left(\frac{2}{B_1} + \frac{1}{B_2}\right) + S^2\left(1 + \frac{2\omega_0}{B_1} + \frac{2\omega_0}{B_2}\right)$$

$$+ S\left(\frac{\omega_0^2}{Q_p} + \frac{\omega_0^2}{B_2}\right) + \omega_0^2 \qquad (3.20b)$$

Writing Eq. (3.20b) as

$$D'(s) \simeq \left(S^2 + \frac{S\omega_{0k}}{Q_{pk}} + \omega_{0k}^2\right)\left\{\left(\frac{2}{B_1} + \frac{1}{B_2}\right)S + \frac{\omega_0^2}{\omega_{0k}^2}\right\} \qquad (3.21)$$

and letting $\omega_{0k} = \omega_0(1 + \delta)$, $\delta << 1$, then comparing S^2-term and S-term coefficients in Eq. (3.21) and Eq.(3.20b) we find

$$\delta \simeq -\left(\frac{\omega_0}{B_1} + \frac{\omega_0}{B_2}\right) \qquad (3.22a)$$

$$= -\frac{2\omega_0}{B} \quad \text{for } B_1 = B_2$$

and

$$\frac{Q_{pk}}{Q_p} = \frac{1}{1 + \delta + \frac{\omega_0}{B_2}(1+\delta)Q_p - Q_p\omega_0(1+3\delta)\left(\frac{2B_2+B_1}{B_1B_2}\right)} \qquad (3.22b)$$

For $B_1 = B_2$

$$\frac{Q_{pk}}{Q_p} = \frac{1}{1 + \delta - 2Q_p \frac{\omega_o}{B} - \frac{8Q_p \omega_o \delta}{B}} \qquad (3.22c)$$

$$\simeq \frac{1}{1 - 2Q_p \frac{\omega_0}{B}} \qquad (3.22d)$$

These results are tabulated in Table 3.2.

3.4 HIGH FREQUENCY STABILITY PROPERTIES

In Section 2.4, it was seen that the circuits derived from Riordan's GIC are free from low frequency unstable modes of operation. In this section, we examine the high frequency stability properties of these circuits.

The results of the last section indicate these circuits exhibit Q_p-enhancement and thus potential instability. More explicitly design A would become unconditionally unstable when

$$7\omega_0 Q_p > 2B \qquad (3.23)$$

and design B becomes unstable when

$$2\omega_0 Q_p > B \qquad (3.24)$$

These conditions impose the absolute upper bound on ω_0 and Q_p that these designs can be realized given a particular Op. Amp.

TABLE 3.2 Q_p, ω_o, DEPENDENCE ON AMPLIFIER GAIN BANDWIDTH B

Design	ω_o	Q_p
A	$\omega_{ok} = \omega_o\left(1 - \frac{3}{2}\frac{\omega_o}{B}\right)$	$\frac{Q_{pk}}{Q_p} = \frac{1}{1 - \frac{7}{2}Q_p\frac{\omega_o}{B}}$
B	$\omega_{ok} = \omega_o\left(1 - \frac{2\omega_o}{B}\right)$	$\frac{Q_{pk}}{Q_p} = \frac{1}{1 - 2Q_p\frac{\omega_o}{B}}$

3.5 COMBINED EFFECT OF R_{in}, R_0 AND A(s) OF OP AMPS

Budak and Zeller [21] have shown that the combined effect of the output impedance, R_0, and the frequency-dependent open loop gain, A(s), of the Op. Amp. might have a limiting effect on the performance of active filters. Differential input impedance of the Op.Amp., R_{in}, also affects adversely filter performance, particularly when element impedances are large.

The controlled source model of a practical Op.Amp. that takes into consideration the differential input impedance, the output impedance and the frequency-dependent gain was shown in Figure 1.1(c) and is redrawn in Figure 3.1(a) for convenience. There are many available circuit analysis computer programs that can be used to study the effect of R_{in}, R_0 and the dc gain A_0 on any active filter design. To incorporate into such analysis the frequency-dependent nature of A(s) the model in Figure 3.1(a) has to be modified.

It was stated earlier that the open loop gain of an internally compensated Op.Amp. such as the μA741 is given as

$$A(s) = \frac{A_0 \omega_c}{S + \omega_c} \quad \frac{A_0}{1 + \frac{S}{\omega_c}} \qquad (1.6)$$

Thus A(s) can be simulated with an RC lowpass network. Consider the circuit shown in Figure 3.1(b). The unity gain amplifier is ideal (i.e. $R_{in} = \infty$, $R_0 = 0$, $B = \infty$).

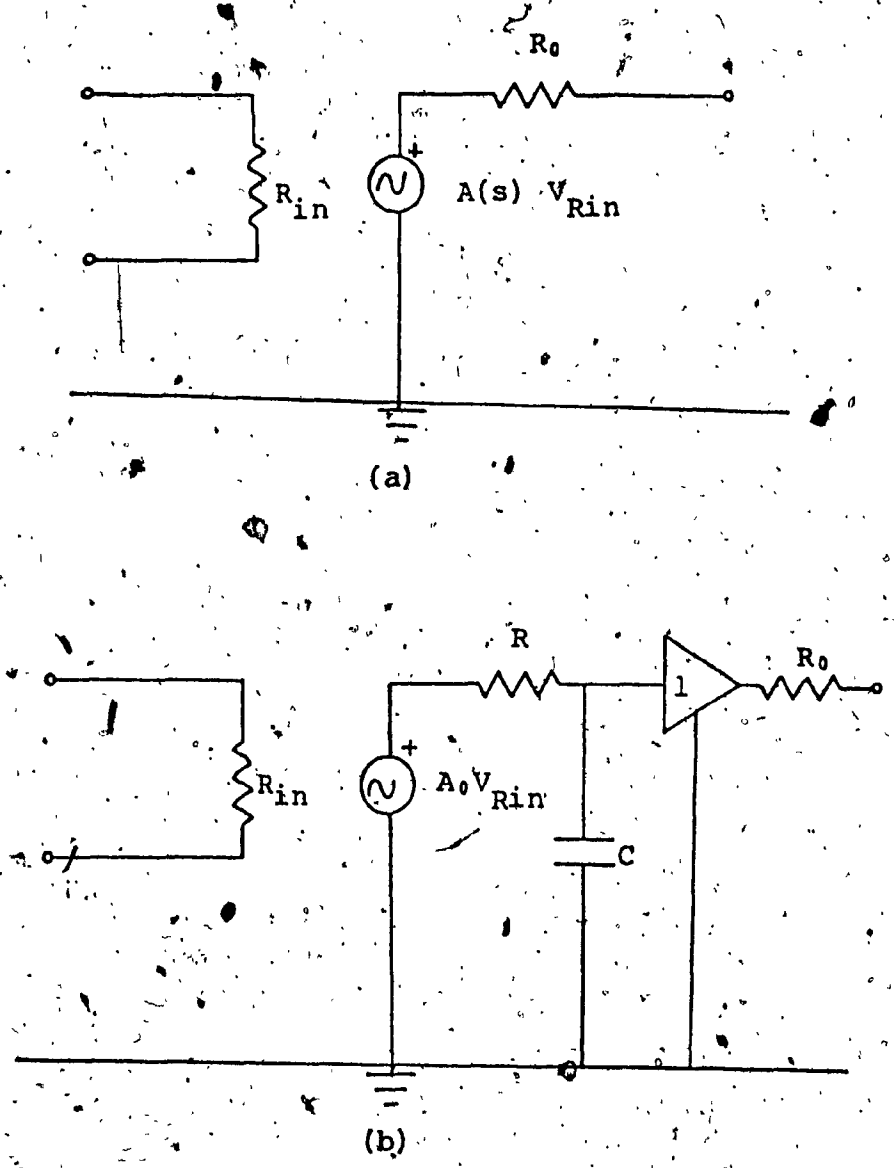

FIG. 3.1 (a) Controlled Source Model of Practical Op.Amp.

(b) Equivalent Controlled Source Model of Practical Op.Amp. Suitable for Computer Simulation

Simple analysis shows that the circuits in Figures 3.1(a) and 3.1(b) are equivalent with respect to the input/output characteristics provided

$$\frac{1}{1 + sRC} = \frac{1}{1 + \frac{S}{\omega_c}} \qquad (3.25a)$$

i.e.,

$$\omega_c RC = 1 \qquad (3.25b)$$

The RC network simulates the frequency dependent portion of A(s) and the unity gain amplifier prevents R_0 from loading the RC network. Thus the circuit of Figure 3.1(b) can be used to model the practical Op.Amp. when using circuit analysis programs.

3.6 EXPERIMENTAL AND SIMULATION RESULTS

In arriving at conclusions about the characteristics of the network designed with Riordan's gyrator, it was necessary to make certain approximations. Thus, in this section we will be mainly concerned with the experimental and simulation verification of analytical results obtained earlier. The experimental and simulation work was conducted in the range 0.5 - 10KHz using the resonator sections. The experimental results were obtained with the Fairchild μA741C Op.Amp. while the simulations used both the μA741 and the μA715. The specifications of these amplifiers are

PARAMETER	μA741C	μA715	UNITS
A_0	200,000	30,000	---
B	1	65	MHz
R_0	75	75	Ω
R_{in}	2	2	MΩ

3.6.1 Results of Measurements on Design B

A resonator section, with a Q-factor of 25 and center frequency of $1KH_z$ using the design values given in Table 2.3 was realized. The Op.Amps. used were the μA741 type (with gain bandwidth of 0.8 MHz), the capacitors were of polystyrene and the resistors were high precision metal film types. The circuit diagram is shown in Figure 3.2.

3.6.1.1 Temperature effects

The filter was built and was tuned (using the tuning sequence given in Table 2.3) to its design values of f_0 and Q_p at $23^{\circ}C$. The results obtained with power supply voltage of ±15V are tabulated below. (f_0 is measured as the frequency where the response peaks; Q_p is then measured by taking those frequencies which are 3dB down from the peak response at f_0.)

f_0 = 1,000 H_z (tuned)

Q_p = 25 (tuned)

Gain at Resonance = 2.10

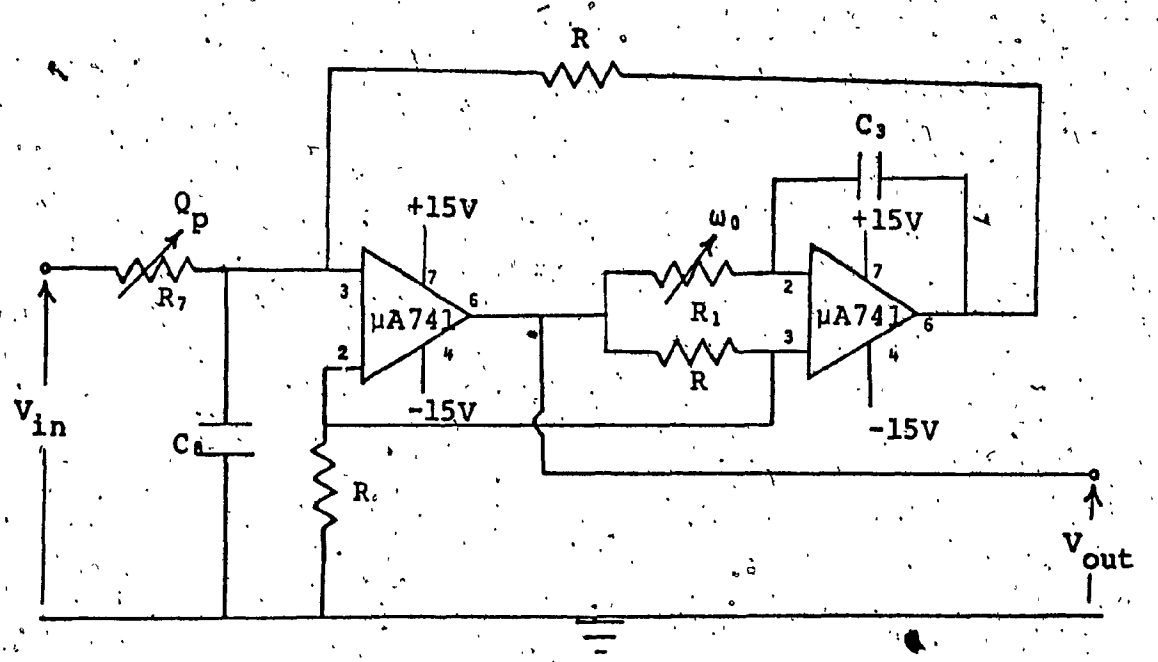

$R = 2K\Omega$

$C_3 = C_8 = C$ $(C = 1/2\pi Rf_0)$

$R_1 = 5K\Omega$ (Variable; for tuning f_0)

$R_7 = 100K\Omega$ (Variable; for tuning Q_p)

$$T(s) = \frac{2\frac{\omega_0}{Q_p}s}{s^2 + \frac{\omega_0}{Q_p}s + \omega_0^2}$$

FIG. 3.2 Realization of Resonator Using Design B

$R_0 < 0.1\Omega$

$R_{in} > 2M\Omega$

The circuit was then put into a temperature chamber and the following measurements were obtained.

RESONATOR (DESIGN B) TEMPERATURE TEST				
	0°C	23°C	40°C	60°C
f_0 (H_z)	998.0	1000	1000.8	1001.1
Q_p	24.4	25.0	25.6	26.3
Gain at f_0	2.06	2.10	2.14	2.18

The above results demonstrate the low sensitivity characteristics of this circuit.

3.6.1.2 Q_p - Enhancement caused by finite gain bandwidth product of Op.Amps.

The limits imposed by the finite bandwidth of Op. Amps. on this design were derived in Section 3.3.2. To verify the analytical expression obtained for the Q_p-enhancement the design value Q_p in the circuit in Figure 3.2 was held constant as f_0 was varied with C_3 and C_8.(Care was taken to make C_3 to be always equal to C_8). The experimental and analytic curves for the actual Q_p of the resonator as a function of the resonant frequency f_0 are given in Figure 3.3. It is noted that the experimental and analytical

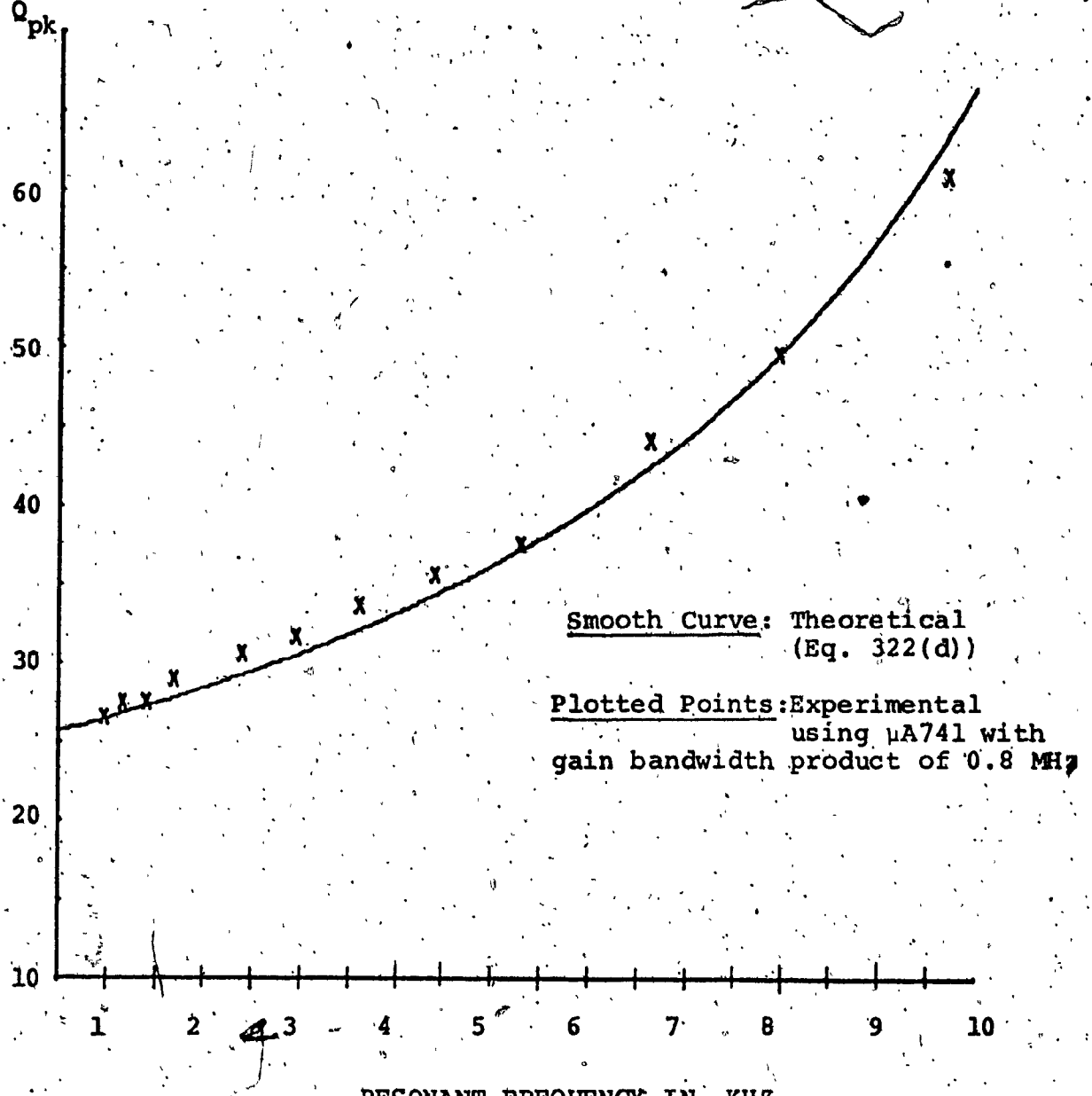

FIG. 3.3 Design B: Actual Q_{pk} of Resonator as Function of Resonant Frequency for Constant Nominal Q_p -Theoretical and Experimental

results are in good agreement.

3.6.2 Simulation Results

When the one pole model as given in Eq. (1.6) is used for the amplifiers, the resulting voltage transfer function for the resonators of Design A and Design B can be written as

$$T(s) = \frac{a_1 s - a_0}{b_4 S^4 + b_3 S^3 + b_2 S^2 + b_1 S + b_0} \qquad (3.26)$$

where, for Design A

$$a_0 = \frac{2\omega_0^2}{A_0 Q_p}$$

$$a_1 = \frac{3\omega_0}{Q_p} - \frac{2\omega_0^2}{Q_p B}$$

$$b_0 = \omega_0^2\left(1 + \frac{1}{2A_0} + \frac{1}{A_0 Q_p} + \frac{3}{2A_0^2} + \frac{3}{2A_0^2 Q_p}\right)$$

$$b_1 = \frac{\omega_0}{Q_p} + \frac{\omega_0}{A_0}\left(3 + \frac{4}{Q_p} + \frac{9}{A_0} + \frac{3\omega_0}{B} + \frac{3}{A_0 Q_p}\right)$$

$$+ \frac{\omega_0^2}{B}\left(\frac{1}{2} + \frac{1}{Q_p} + \frac{6}{A_0 Q_p}\right)$$

$$b_2 = 1 + \frac{4}{A_0} + \frac{3}{A_0^2} + \frac{\omega_0}{A_0 B}\left(9 + \frac{6}{Q_p}\right) + \frac{\omega_0}{B^2 Q_p}(3BQ_p + 4B$$

$$+ 1.5\omega_0 Q_p + 3\omega_0)$$

$$b_3 = \frac{4}{B} + \frac{7\omega_0}{2B^2} + \frac{3\omega_0}{B^2 Q_p} + \frac{6}{A_0 B}$$

$$b_4 = \frac{3}{B^2} \qquad (3.27)$$

and for Design B

$$a_0 = \frac{\omega_0^2}{A_0 Q_p}$$

$$a_1 = \frac{2\omega_0}{Q_p} - \frac{\omega_0^2}{Q_p B}$$

$$b_0 = \omega_0^2\left(1 + \frac{1}{A_0} + \frac{1}{A_0 Q_p} + \frac{2}{A_0^2} + \frac{1}{A_0^2 Q_p}\right)$$

$$b_1 = \frac{\omega_0}{Q_p} + \frac{\omega_0}{A_0}\left(4 + \frac{3}{Q_p} + \frac{4}{A_0} + \frac{4\omega_0}{B} + \frac{2}{A_0 Q_p}\right) +$$

$$+ \frac{\omega_0^2}{B}\left(1 + \frac{1}{Q_p} + \frac{4}{A_0 Q_p}\right)$$

$$b_2 = 1 + \frac{3}{A_0} + \frac{3}{A_0^2} + \frac{\omega_0}{A_0 B}\left(8 + \frac{4}{Q_p}\right) + \frac{\omega_0}{B Q_p}(4BQ_p + 3B +$$

$$+ 2\omega_0 Q_p + 2\omega_0)$$

$$b_3 = \frac{3}{B} + \frac{4\omega_0}{B^2} + \frac{2\omega_0}{B^2 Q_p} + \frac{4}{A_0 B}$$

$$b_4 = \frac{2}{B^2} \qquad (3.28)$$

To study the exact effects of A_0 and B on the pole-Q, pole frequency and the gain at resonance for any particular resonator design, Eq.(3.26) has to be simulated on a digital computer. This was done (using the programs in Appendix A and B) using the nominal values for Fairchild μA741 and μA715 Op. Amps, for Q_p and f_0 ($= \frac{\omega_0}{2\pi}$) in the range (25-100) and (1000-10,000 H_z). The results of the simulations are given in Figs. 3.4-3.7. It is observed that as the resonant frequency

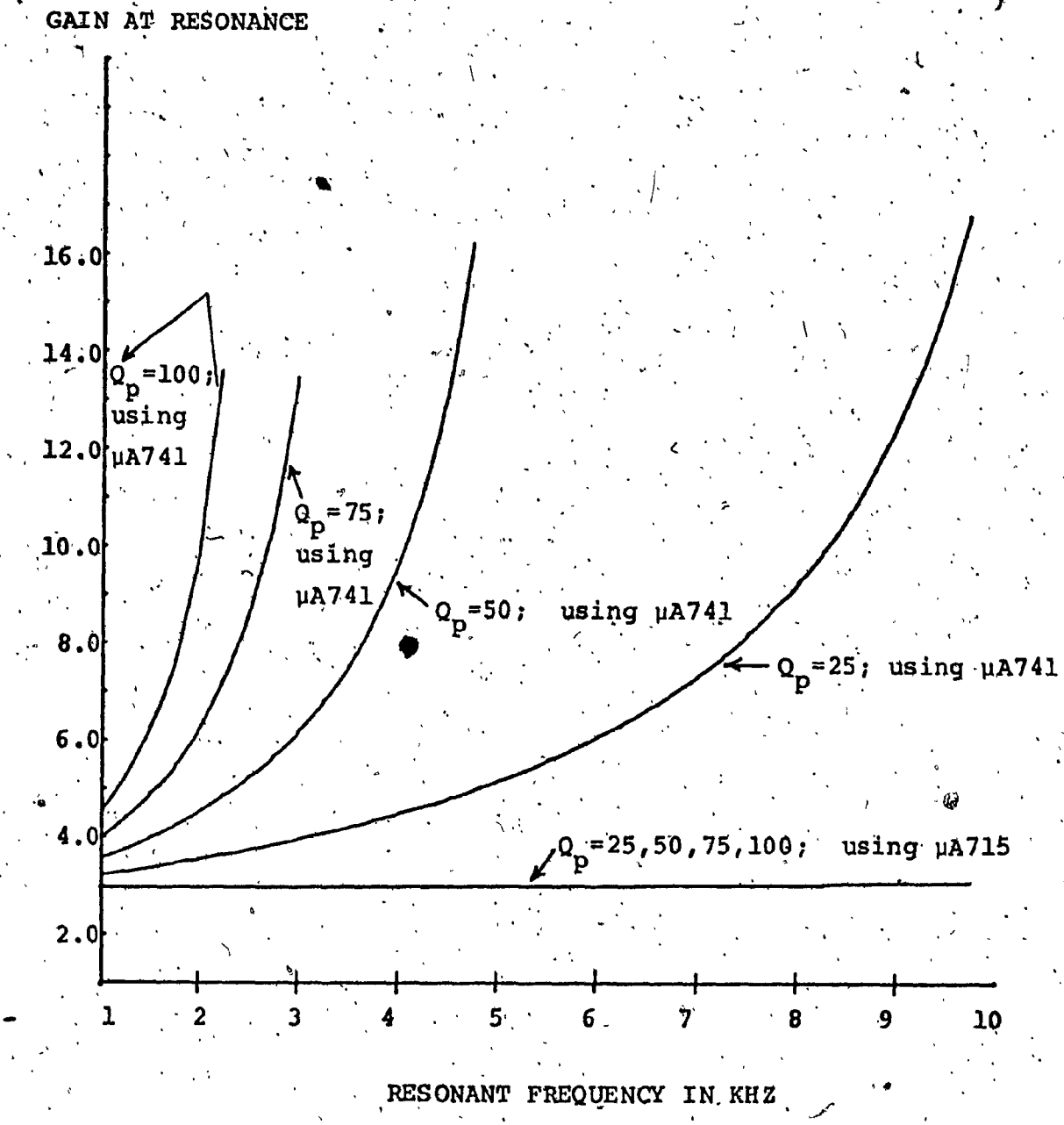

FIG. 3.4 Design A - Actual Gain at Resonance of Resonator as Function of Resonant Frequency: Simulated

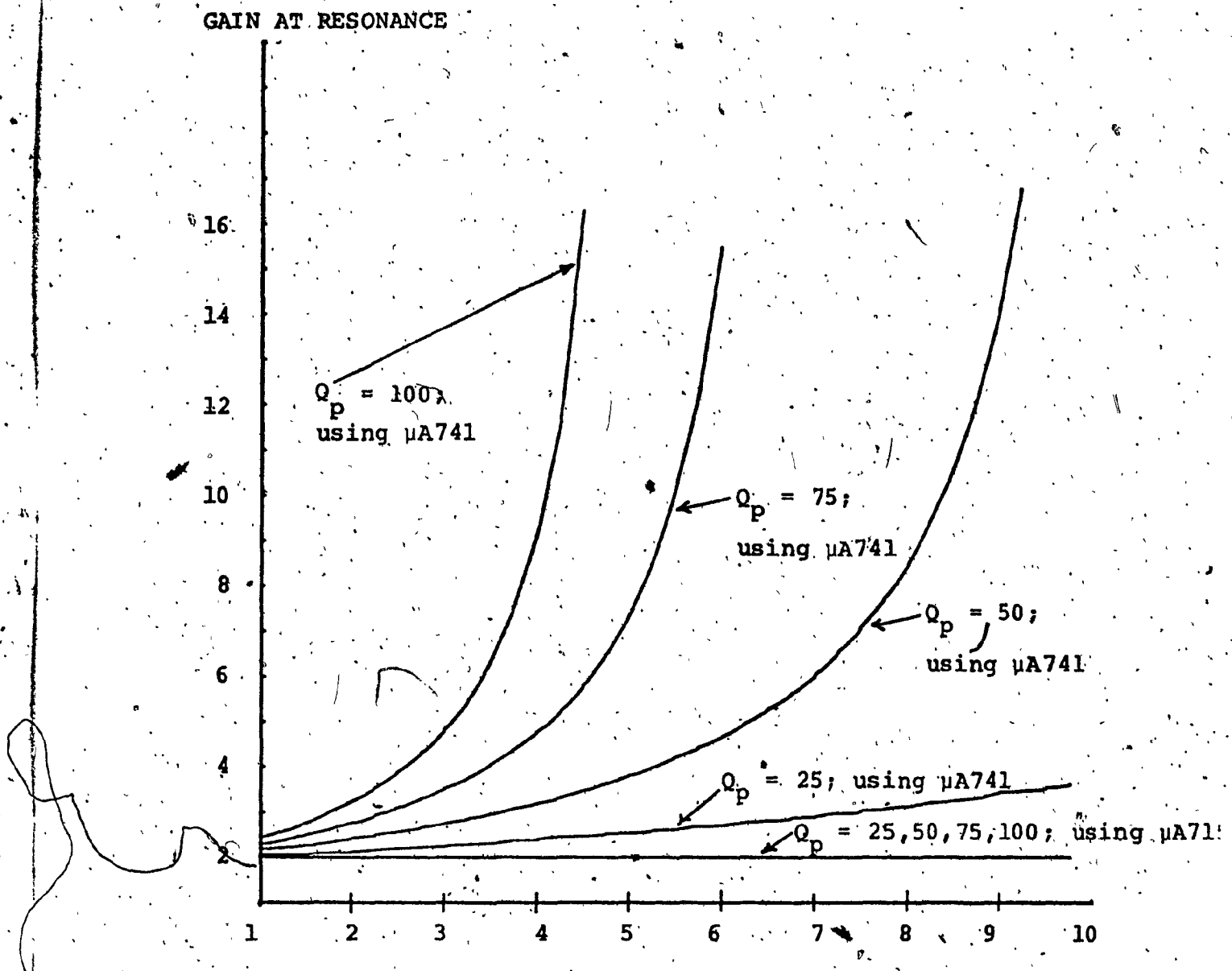

FIG. 3.5 Design B - Actual Gain at Resonance of Resonator as Function of Resonant Frequency: Simulated

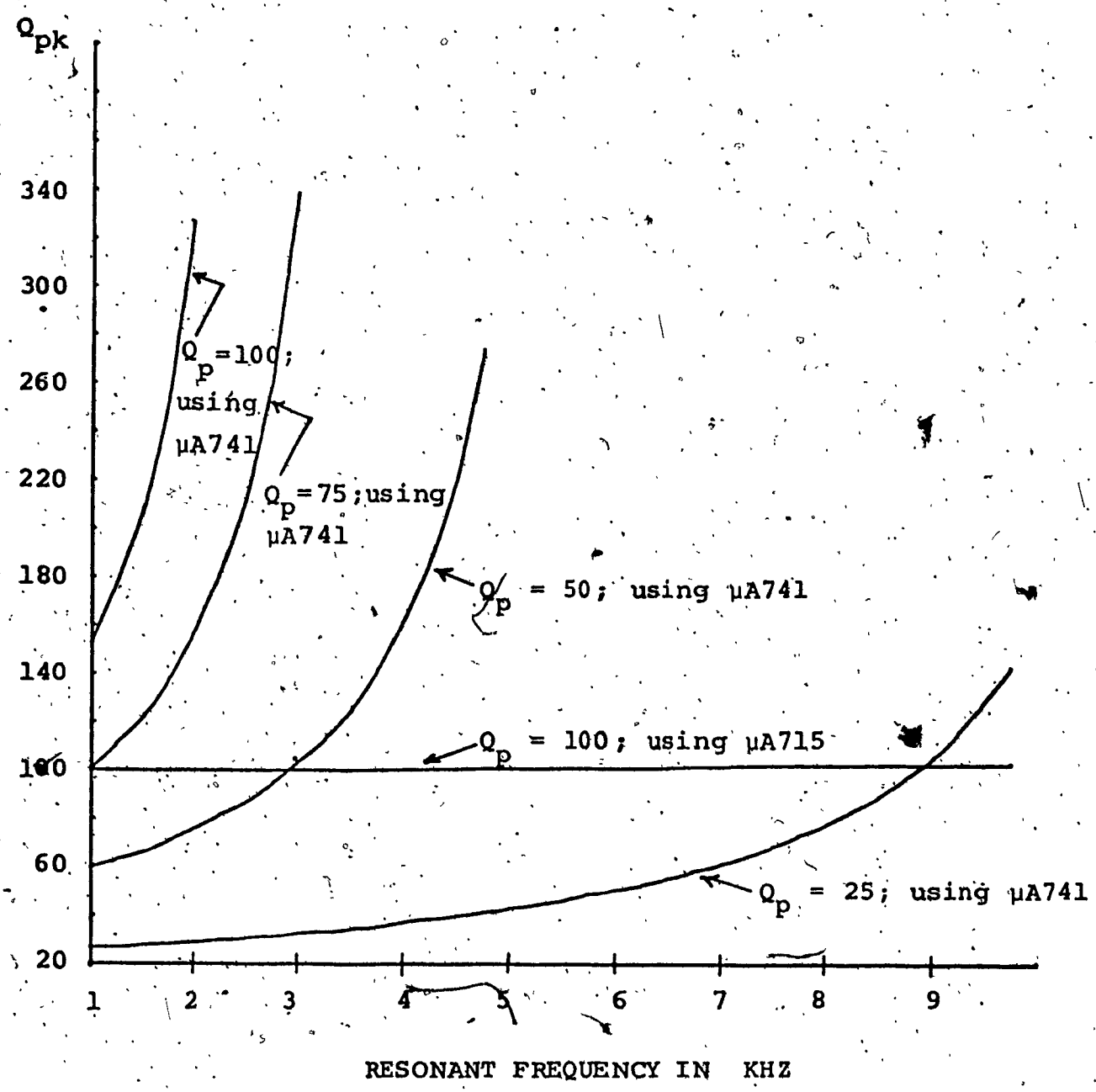

FIG. 3.6 Design A - Actual Q_p of Resonator as Function of Resonant Frequency: Simulated

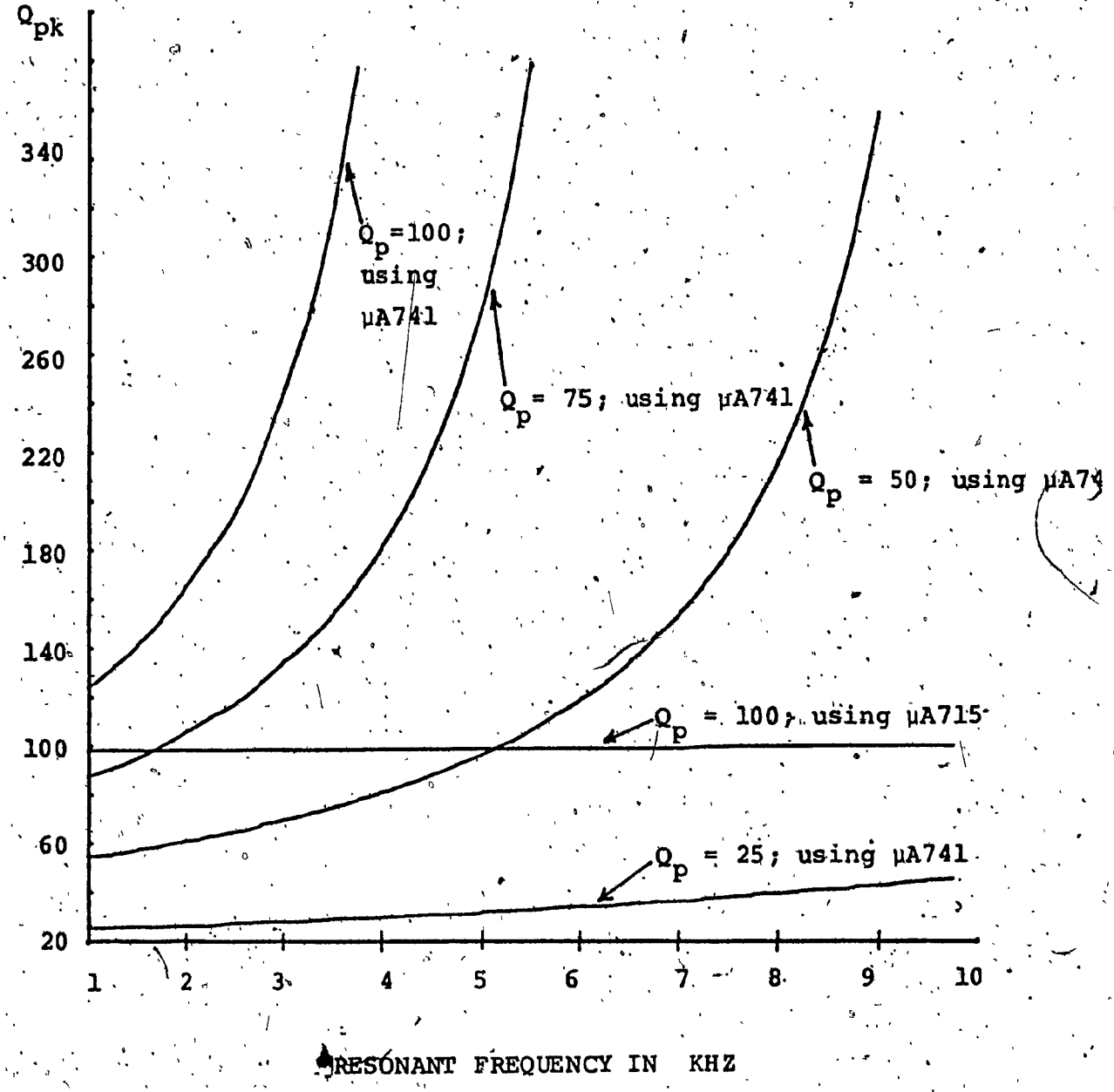

FIG. 3.7 Design B - Actual Q_p of Resonator as Function of Resonant Frequency: Simulated

increases there is enhancement in the pole Q and the gain at resonance of the circuit. The gain at resonance becomes very pronounced with higher Q_p values. The shift in f_0 was negligible.

The difference in the results for the μA741 and μA715 illustrate that the limiting factor in this circuit is the gain bandwidth product of the Op.Amps.

3.6.3 Effect of Op.Amps. Input and Output Resistances

Eq. (3.26) takes into account the finite open loop given of the Op.Amps. In addition to the limitations imposed by finite open loop gain, the input and output resistance of the Op.Amps. may further limit the usefulness of the resonators. To estimate the effect of the differential input resistance and output resistances of the Op.Amps., the circuit in Fig. 3.2 was studied for Q_p in the range 25-100 and for f_0 varying from 1000-10,000 Hz. The Op.Amps. were replaced by the model given in Fig. 3.1 and the KRON AC NETWORK ANALYSIS PROGRAM at the Concordia University Computer Center was used to analyze the circuit. The results of the analysis indicate that the pole Q, resonant frequency and the gain at resonance were within 0.7% of those obtained from Eq. (3.26).

3.7 CONCLUSION

The behaviour of the network when using non-ideal Op. Amps. was analysed and theoretical expressions were obtained for the limitations imposed by the Op.Amps. Experimental and simulations results corresponded closely to the theoretical predictions.

CHAPTER IV

COMPARISONS, SUMMARY AND CONCLUSIONS

4.1 INTRODUCTION

This Chapter presents a detailed comparison of performances of the biquadratic sections designed in Chapter II with other two-amplifier realizations that have been found to be very promising. The figures-of-merit are the ω_0 and the Q_p-sensitivities. In addition to the sensitivities, the limiting effect of the amplifier finite band-width on filter response, expressed through the shift in ω_0 and Q_p, is also compared for these circuits.

Other practical considerations such as component spread, tunability and cascadability, important in selecting a biquadratic section, are also considered for these circuits.

4.2 EXISTING PROMISING TWO-AMPLIFIER BIQUADRATIC NETWORKS

In a recent study [14] reported by Sedra and Espinoza two networks have emerged as the 'best' two-amplifier realizations of biquadratic functions. In fact only these two circuits seem to offer any advantage over their single amplifier counterpart. These two circuits are based on the idea of GIC's. The general properties of these circuits are discussed below.

4.2.1 Sedra and Hamilton (SH) Circuit

The network shown in Figure 4.1 was presented by Sedra and Hamilton [18]. This circuit is based on the original structure of Riordan's [9] inductance simulation circuit and later classified by Bruton [19] as Class B2 of FIC's.

For the circuit values given by the authors the voltage transfer function is given by

$$T(s) = \frac{(K_2+1)\frac{\omega_0}{Q_p}S + \frac{\omega_0^2}{Q_p}}{S^2(K_2+1) + S(K_2\frac{\omega_0}{Q_p} + \frac{\omega_0}{Q_p} + 2\omega_0) + \omega_0^2(K_1K_2 - K_2 + 1 + \frac{1}{Q_p})} \qquad (4.1)$$

For $K_1 = 2$ and $K_2 \to \infty$, this circuit realizes a resonator with the transfer function given by

$$T(s) = \frac{\frac{\omega_0}{Q_p}S}{S^2 + \frac{\omega_0}{Q_p}S + \omega_0^2} \qquad (4.2)$$

Also for the equal capacitor design and for ideal amplifiers

$$\omega_0 = (R_3R_4C^2)^{-\frac{1}{2}} \qquad (4.3a)$$

$$Q_p = R_1(R_3R_4)^{-\frac{1}{2}} \qquad (4.3b)$$

Thus the requirements for tunability are met. (By using R_3 or R_4 for adjusting ω_0 and R_1 for adjusting Q_p in that sequence.)

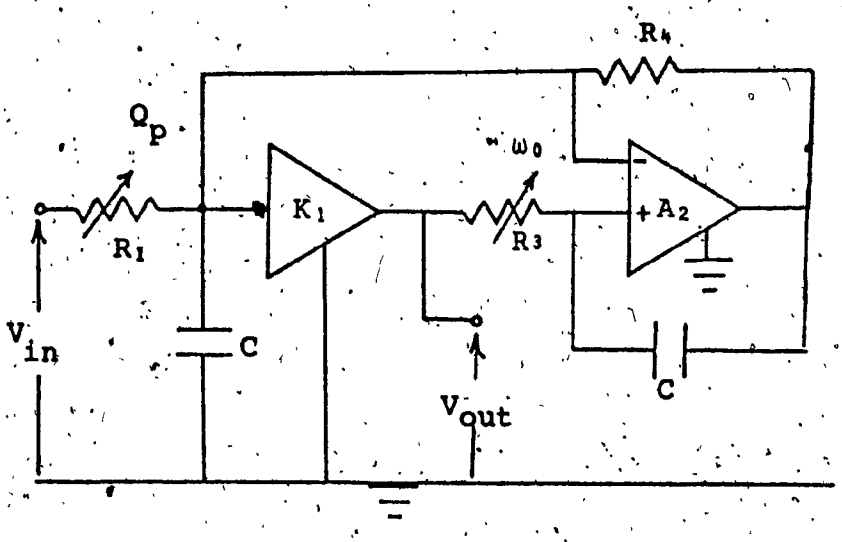

$K_1 = 2$

$A_2 = K_2$

$R_3 = R_3 = R$

$R_1 = Q_p R$

$\omega_0 CR = 1$

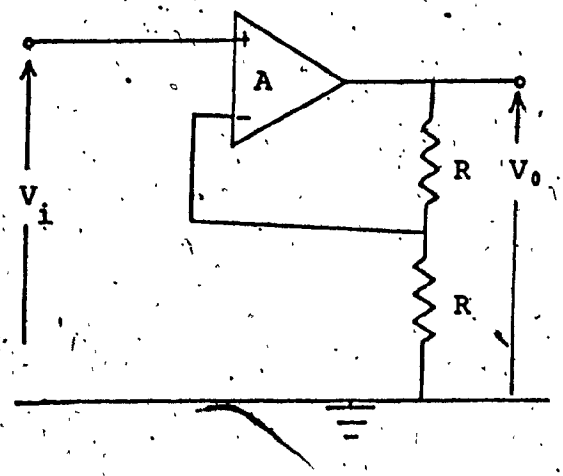

FIG. 4.1 (a) Sedra-Hamilton Realization of Gyrator from Riordan Gyrator

(b) Op. Amp. Realization of K_1

The sensitivities of ω_0 and Q_p to passive elements variation are all equal to or less than one.

We now look at the non-ideal behaviour of this network. For non-ideal Op.Amps. with a one-pole frequency response we obtain

$$K_1 = \frac{2}{1 + \frac{2}{A_{01}} + \frac{S}{B_1}} \qquad (4.4a)$$

$$K_2 = \frac{A_{02}\,\omega_c}{S + \omega_c} \qquad (4.4b)$$

At low frequencies such that the gains of amplifiers are real but finite numbers we have

$$K_1 = \frac{2}{1 + \frac{2}{A_{01}}} \qquad (4.5a)$$

$$K_2 = A_{02} \qquad (4.5b)$$

By substituting Eq. (4.5) in Eq. (4.1) we can show that

$$S_{A_0}^{\omega_0} \approx 0 \qquad (4.6a)$$

and

$$S_{A_0}^{Q_p} \approx 2\frac{Q_p}{A_0} \qquad (4.6b)$$

when $A_{01} \approx A_{02} >> 1$.

It should be noted that this circuit can attain a low frequency unstable mode of operation, as the denominator polynomial contains a negative term. Since the amplifier gains rise from zero (just after switching on the power supply) in an uncorrelated manner, we will now show that attainable sets of amplifier gains exist which will make this circuit unstable. For example, for $A_{01} = 0.5$, $A_{02} = 4$, we have from Eq. (4.5) $K_1 = 0.4$ and $K_2 = 4$. Substituting these gain values in Eq. (4.1) we obtain

$$T(s) = \frac{5\frac{\omega_0}{Q_p}S + \frac{\omega_0^2}{Q_p}}{5S^2 + S(\frac{5\omega_0}{Q_p} + 2\omega_0) + \omega_0^2(\frac{1}{Q_p} - 1.4)} \qquad (4.7)$$

By applying the Routh-Hurwitz stability criterion it is found that for $Q_p > 0.714$ the circuit is unstable for this set of Op.Amp. gains.

To obtain the shifts in ω_0 and Q_p due to the excess phase introduced by the Op.Amps we substitute Eq.(4.4) in Eq. (4.1) and use the method of Section 3.3 of Chapter III to evaluate these quantities. We find, for identical Op.Amps., that

$$\frac{Q_{pk}}{Q_p} = \frac{1}{1 - 4Q_p\frac{\omega_0}{B}} \qquad (4.8a)$$

and

$$\omega_{0_k} = \omega_0(1 - \frac{\omega_0}{B}) \qquad (4.8b)$$

Thus this circuit exhibits Q_p enhancement and thus is limited to low frequency operation (i.e., $\omega_o << B$).

4.2.2 Bhattacharyya, Mikhael and Antoniou (BMA) Circuit

The network shown in Figure 4.2 was presented by Bhattacharyya et al [20] and its properties have been extensively studied in [13]. This circuit is derived from the Antoniou [8] inductance simulation circuit which belongs to Class A1 of Bruton's [19] classification of PIC's.

The voltage transfer function of this circuit is

$$T(s) = \frac{2\frac{\omega_o}{Q_p}s}{s^2\left(1+\frac{2}{A_2}+\frac{2}{A_1A_2}\right)+s\frac{\omega_o}{Q_p}\left[1+\frac{2}{A_2}+\frac{2}{A_1A_2}+2Q_p\left(\frac{1}{A_1}+\frac{1}{A_2}+\frac{2}{A_1A_2}\right)\right]+\omega_o^2\left[1+\frac{2}{A_1}+\frac{1}{A_1Q_p}\left(1+\frac{1}{A_2}\right)\right]}$$

It is shown in [13] that for $A_1 \simeq A_2$ and $A_0 >> 1$,

$$S_{A_0}^{\omega_o} \simeq -\frac{1}{A_0 Q_p} \simeq 0 \qquad (4.10a)$$

$$S_{A_0}^{Q_p} \simeq \frac{4Q_p}{A_0} \qquad (4.10b)$$

The Q_p and ω_o passive sensitivities are all equal or less than one. It should be noted that this circuit is absolutely stable at low frequencies. The tuning of the circuit is straightforward, using only resistors, as indicated in Figure 4.2.

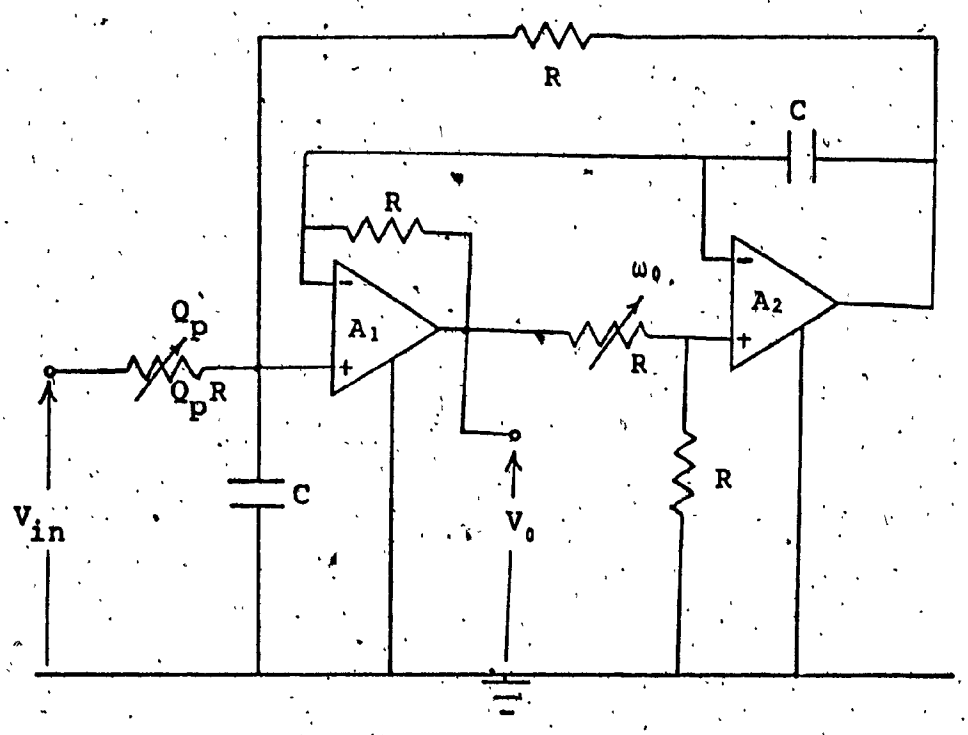

FIG. 4.2 Resonator Realization Using Antoniou's GIC [20].

The ω_0 and Q_p shifts due to amplifier bandwidth limitations are given by

$$\omega_{0_k} = \omega_0\left(1 - \frac{2\omega_0}{B}\right) \qquad (4.11a)$$

and

$$\frac{Q_{pk}}{Q_p} = \frac{1}{1 - \frac{2\omega_0}{B} + 8Q\frac{\omega_0^2}{B^2}} \qquad (4.11b)$$

It is seen that this circuit does not exhibit Q_p enhancement as is the case with the other circuits. The phase shift in one amplifier tends to cancel the effect of phase shift in the other amplifier.

4.3 COMPARISON WITH BMA AND SH REALIZATIONS

The salient features of the proposed design are listed in Table 4.1 along with those of the other realizations just described. The assumption made in deriving the different properties is that identical Op. Amps. are used in all the realizations. The low frequency sensitivities for these circuits are seen to be of the same order of magnitude for all the realizations. While the proposed designs and the BMA realization are absolutely stable in the region where $\omega_0 << B$, the SH realization is potentially unstable at low frequencies. In the high frequency region the proposed designs, as well as the SH realization show Q_p-enhancement which can lead to instability. However, the Q_p-enhancement is most rapid in the

TABLE 4.1 COMPARATIVE PROPERTIES OF GIC FILTERS

Network		$\omega_s \ll B$				Effect of Op.Amp. Bandwidth		$\frac{C_{max}}{C_{min}}$	Resistor Values Req'd	Tuning Properties	Stability Properties
		$\lvert S^{Q_p}_{R,C} \rvert$	$\lvert S^{\omega_o}_{R,C} \rvert$	$S^{Q_p}_{A_o}$	$S^{\omega_o}_{A_o}$	Q_{pk}/Q_p =	ω_{ok}/ω_o =				
Proposed Design (Riordan's GIC)	Design A	≤ 1	$\leq \frac{1}{2}$	$\frac{3Q_p}{A_o}$	$\frac{7}{4A_o} \neq 0$	$\frac{1}{1 - 3.5Q_p\frac{\omega_s}{B}}$	$1 - 1.5\frac{\omega_s}{B}$	1	R, 2R, RQ_p	Easy, in sequence of ω_s, Q_p using resistors only	Absolutely stable for $\omega_s \ll B$. Possibility of high frequency instability caused by excess phase of Op.Amp.
	Design B	≤ 1	$\leq \frac{1}{2}$	$\frac{4Q_p}{A_o}$	$\frac{1}{A_o} \neq 0$	$\frac{1}{1 - 2Q_p\frac{\omega_s}{B}}$	$1 - \frac{2\omega_s}{B}$	1	R, RQ_p	Same as above	Same as above
Hamilton & Sedra (Riordan's GIC)		≤ 1	$\leq \frac{1}{2}$	$\frac{2Q_p}{A_o}$	$\neq 0$	$\frac{1}{1 - 4Q_p\frac{\omega_s}{B}}$	$1 - \frac{\omega_s}{B}$	1	R, RQ_p	Same as above	Conditionally unstable for $\omega_s \ll B$. Possibility of instability at moderately high ω_s.
Bhattacharyya, Mikhael and Antoniou (Antoniou GIC)		≤ 1	$\leq \frac{1}{2}$	$\frac{4Q_p}{A}$	$-\frac{1}{A}Q_p \neq 0$	$\frac{1}{1 - \frac{2\omega_s}{B} + 8Q\frac{\omega_s^2}{B^2}}$	$1 - \frac{2\omega_s}{B}$	1	R, RQ_p	Same as above	Absolutely stable both at low and high ω_s.

SH realization.† The BMA realization shows no such tendency since it does not exhibit Q_p-enhancement.

While the resistor spread is the same for all the realizations, Design A of the proposed realization requires three different values of resistors. For the same capacitance value, this also makes the total resistance in the section equal to $R(6 + Q_p)$ while for the other sections this is equal to $R(4 + Q_p)$. The fact that Design A requires three different values of resistors as compared to two in the other realizations is an inventory problem when using discrete component construction. Furthermore, the higher total resistance is a disadvantage in integrated circuit fabrication since this will require more substrate area.

It is also observed that the cascading and tuning properties for all these realizations are alike.

4.4 CONCLUSIONS

In this work an RC-active filter design technique using the stable form of Riordan's GIC has been described and studied at length. It is shown that a number of universal second-order sections (LP,BP,HP,AP,N), suitable for cascade synthesis, are obtainable from the basic structure. The

---

† For a given Op.Amp. and Design Q_p.

network characteristics (Q_p, ω_0) of these sections exhibit low sensitivity to both passive and active element variations. The tuning of the section is simple and uses only resistors for this purpose. Among all the second-order sections derived from this configuration only the notch section requires an isolating amplifier when there is need to cascade the sections to obtain higher order filters.

These filter sections also exhibit freedom from low frequency unstable mode of operation. However, the one drawback of these sections is the Q_p-enhancement caused by the excess phase introduced by the Op.Amps. Other second order effects such as Op.Amp. Input/Output resistance on filter performance were simulated and found to be negligible.

Comparison with other two-amplifier biquads show that the sections designed in this work exhibit many favorable results. As a matter of fact, the resonator section shows a definite improvement over the SH two-amplifier biquad while its only drawback as compared to the BMA resonator is Q_p - enhancement.

In conclusions, the author hopes that the results of the investigations carried out in this work would prove useful in active filter design.

REFERENCES

[1] L.P.Hullsman,Ed., Active Filters: Lumped,Distributed, Integrated,Digital and Parametric, New York: McGraw-Hill, 1970.

[2] S.K.Mitra, Ed., Active Inductorless Filters, IEEE Press, 1971.

[3] A.Antoniou, "Novel RC-Active Network Synthesis Using Generalized Immittance Converters", IEEE Trans-Circuit Theory, Vol. CT-17, May 1970.

[4] H.J. Orchard, "Inductorless Filters", Electronic Letters, Vol. 2, September, 1966.

[5] L.T. Bruton, "Network Transfer Functions Using the Concept of Frequency-Dependent Negative Resistance", IEEE Trans. CT, Vol. CT,16, No. 3, August, 1969.

[6] S.K. Mitra, Analysis and Synthesis of Linear Active Networks, New York: Wiley, 1969.

[7] G. Martinelli, "Comments on Nullor Model of the Transistor", Proc. IEEE, 53, July 1965.

[8] A. Antoniou, "Realization of Gyrators Using Operational Amplifiers and Their Use in RC-active Network Synthesis", Proc. IEE, 116, November, 1969.

[9] R.H.S.Riordan, "Simulated Inductors Using Differential Amplifiers", Electronic Letters, Vol. 3, February, 1967.

[10] A. Antoniou, "Stability Properties of Some Gyrator Circuits", Electronic Letters, Vol. 4, November, 1968.

[11] D. Hilberman, "An Approach to the Sensitivity and Statistical Variability of Biquadratic Filters", IEEE, Trans-CT, Vol. CT-20, July, 1973.

[12] B.A.Shenoi, "On a New Statistical Variability Criterion for Optimal Design and Comparative Evaluation of RC-Active Filters", IEEE International Symposium on Circuit Theory, Toronto, Proceedings, 1973.

[13] W.B. Mikhael, "Design of High Performance RC-Active Filters", D.Eng. Thesis, Sir George Williams University, Montreal, May, 1973.

[14] A.S. Sedra and J.L.Espinoza, "Sensitivity and Frequency Limitations of Biquadratic Active Filters", IEEE Trans. Circuits and Systems, Vol. CAS-22, No.2, February, 1975.

[15] L.T. Bruton, "Biquadratic Sections Using Generalized Impedances Converters", The Radio and Electronic Engineer, Vol.41, No.11, 1971.

[16] J.Valihora and J.T.Lim, "The Feasibility of Active Filtering in Frequency Division Multiplex Systems", IEEE International Symposium on Circuits and Systems, San Francisco, Calif., April, 1974.

[17] A.Budak and D.M.Petrela, "Frequency Limitations of Active Filters Using Operational Amplifiers", IEEE Trans-CT, Vol. CT-19, July, 1972.

[18] T.A. Hamilton and A.S. Sedra, "A Novel Application of a Gyrator-Type Circuit", Fifth Asilomar Conference on Circuits and Systems, Conf. Rec., 1971.

[19] L.T. Bruton, Non-Ideal Performance of Two-Amplifier Positive Impedance Converters", IEEE Trans. CT, Vol.CT-17, November, 1970.

[20] B.B. Bhattacharrya, W.B. Mikhael and A. Antoniou, "Design of RC-Active Networks Using Generalized-Immittance Converters", Journal of the Franklin Institute, Vol.297, No. 1, January, 1974.

[21] A. Budak and E.R.Zeller, "Practical Design Considerations for a Variable Center Frequency, Constant Band-Width and Constant Peak-Value Filter", IEEE Journal of Solid-State Circuits, Vol.SC-7,August, 1972.

APPENDIX A

COMPUTER PROGRAMS FOR CALCULATING THE EXACT VALUES OF Q_{pk}, ω_{0_k} AND GAIN OF RESONATOR SECTION OF DESIGN A IMPLEMENTED USING μA741 AND μA715 OP.AMPS. FOR DIFFERENT VALUES OF Q_p AND ω_0

```
      PROGRAM DFSA(INPUT,OUTPUT)
C     *  EFFECT OF OP. AMP. IMPERFECTIONS ON DESIGN A *
C     *  OP=20 TO 100, FO = 1KHZ TO 10KHZ*
C     *  TYPE 741 OP. AMP. *
      DIMENSION XCOF(5),COF(5),ROOTR(5),ROOTI(5)
      M=4
      B=2.*3.14159*1000000.
      A0=200000.
      DO 3 NQ=25,100,25
      QP=NQ
      DO 1 I=1000,10000,250
      FP=I
      WO=2.*3.14159*FP
      XCOF(1)=WO*WO*(1.+0.5/A0+1./(A0*QP)+1.5/(A0*A0)+1.5/(A0*A0*QP))
      XCOF(2)=WO/QP+WO/A0*(3.+4./QP+9./A0+3.*WO/B+3./(A0*QP))
     1+WO*WO/B*(0.5+1./QP+6./(A0*QP))
      XCOF(3)=1.+4./A0+3./(A0*A0)+WO/(A0*B)*(9.+6./QP)+
     1WO/(B*B*QP)*(3.*B*QP+4.*B+1.5*WO*QP+3.*WO)
      XCOF(4)=4./B+3.5*WO/(B*B)+3*WO/(B*B*QP)+6./(A0*B)
      XCOF(5)=3./(B*B)
      CALL POLRT(XCOF,COF,M,ROOTR,ROOTI,IER)
      WPACT=(ROOTI(1)**2+ROOTR(1)**2)**0.5
      QPACT=(-1.)*WPACT /(2.*ROOTR(1))
      B1=(XCOF(5)*(WPACT**4)-XCOF(3)*(WPACT**2)+XCOF(1))**2
      B2=(XCOF(2)*WPACT-XCOF(4)*(WPACT**3))**2
      A1=(2.*(WO*WO)/(A0*QP))  **2
      A2=((3.*WO/QP-2.*WO*WO/(QP*B))*WPACT)**2
      GAIN=((A1+A2)/(B1+B2))**0.5
      FPACT=WPACT/(2.*3.14159)
      DEVQP=(QPACT-QP)/QP
      DEVFP=(FPACT-FP)/FP
      PRINT4,QP,QPACT,DEVQP,GAIN
    4 FORMAT(4X,*QP=*,F7.1,4X,*QPACT=*,F10.4,4X,*DEVQP=*,F10.4,4X,*GAIN=
     1*,F7.4)
      PRINT 5,FP,FPACT,DEVFP
    5 FORMAT(4X,*FP=*,F12.0,4X,*FPACT=*,F12.2,4X,*DEVFP=*,F14.6)
      PRINT6,(ROOTR(J),ROOTI(J), J=1,4)
    6 FORMAT(4X,*REAL  PART=*,E16.7,6X,*IMAG PART=*,F20.7,/)
    1 CONTINUE
    3 CONTINUE
      STOP
      END
```

```
      PROGRAM DESA(INPUT,OUTPUT)
C     * EFFECT OF OP. AMP. IMPERFECTIONS ON DESIGN A *
C     * OP=20 10 100, FO = 1KHZ TO 10KHZ*
C     *  TYPE 715 OP.AMP. *
      DIMENSION XCOF(5),COF(5),ROOTR(5),ROOTI(5)
      M=4
      B=2.*3.14159*65000000.
      AO=30000.
      DO 3 NO=25,100,25
      OP=NO
      DO 1 I=1000,10000,250
      FP=I
      WO=2.*3.14159*FP
      XCOF(1)=WO*WO*(1.+0.5/AO+1./(AO*OP)+1.5/(AO*AO)+1.5/(AO*AO*OP))
      XCOF(2)=WO/OP+WO/AO*(3.+4./OP+9./AO+3.*WO/B+3./(AO*OP))
     1+WO*WO/B*(0.5+1./OP+6./(AO*OP))
      XCOF(3)=1.+4./AO+3./(AO*AO)+WO/(AO*B)*(9.+6./OP)+
     1WO/(B*B*OP)*(3.*B*OP+4.*B+1.5*WO*OP+3.*WO)
      XCOF(4)=4./B+3.5*WO/(B*B)+3*WO/(B*B*OP)+6./(AO*B)
      XCOF(5)=3./(B*B)
      CALL POLRT(XCOF,COF,M,ROOTR,ROOTI,IER)
      WPACT=(ROOTI(1)**2+ROOTR(1)**2)**0.5
      OPACT=(-1.)*WPACT/(2.*ROOTR(1))
      B1=(XCOF(5)*(WPACT**4)-XCOF(3)*(WPACT**2)+XCOF(1))**2
      B2=(XCOF(2)*WPACT-XCOF(4)*(WPACT**3))**2
      A1=(2.*(WO*WO)/(AO*OP))**2
      A2=((3.*WO/OP-2.*WO*WO/(OP*B))*WPACT)**2
      GAIN=((A1+A2)/(B1+B2))**0.5
      FPACT=WPACT/(2.*3.14159)
      DEVOP=(OPACT-OP)/OP
      DEVFP=(FPACT-FP)/FP
      PRINT4,OP,OPACT,DEVOP,GAIN
    4 FORMAT(4X,*OP=*,F7.1,4X,*OPACT=*,F10.4,4X,*DEVOP=*,F10.4,4X,*GAIN=
     1*,F7.4)
      PRINT 5,FP,FPACT,DEVFP
    5 FORMAT(4X,*FP=*,F12.0,4X,*FPACT=*,F12.2,4X,*DEVFP=*,F14.6)
      PRINT6,(ROOTR(J),ROOTI(J), J=1,4)
    6 FORMAT(4X,*REAL PART=*,E16.7,6X,*IMAG PART=*,E20.7,/)
    1 CONTINUE
    3 CONTINUE
      STOP
      END
```

APPENDIX B

COMPUTER PROGRAMS FOR CALCULATING THE EXACT VALUES OF Q_{pk}, ω_{0k} AND GAIN OF RESONATOR SECTION OF DESIGN B IMPLEMENTED USING μA741 AND μA715 OP.AMPS. FOR DIFFERENT VALUES OF Q_p AND ω_0

```
      PROGRAM DESB(INPUT,OUTPUT)
C  *  EFFECT OF OP. AMP. IMPERFECTIONS ON DESIGN B *
C  *  OP=20 TO 100, FO = 1KHZ TO 10KHZ*
C  *  TYPE 741 OP. AMP. *
      DIMENSION XCOF(5),COF(5),ROOTR(5),ROOTI(5)
      M=4
      B=2.*3.14159*1000000.
      AO=200000.
      DO 3 NO=25,100,25
      OP=NO
      DO 1 I=1000,10000,250
      FP=I
      WO=2.*3.14159*FP
      XCOF(1)=WO*WO*(1.+1./AO+1./(AO*OP)+2./(AO*AO)+2./(AO*AO*OP))
      XCOF(2)=WO/OP+WO/AO*(4.+3./OP+4./AO+4.*WO/B+2./(AO*OP))
     1+WO*WO/B*(1.+1./OP+4./(AO*OP))
      XCOF(3)=1.+3./AO+3./(AO*AO)+WO/(AO*B)*(B.+4./OP)+WO/(B*B*OP)*
     1(4.*B*OP+3.*B+2.*WO*    OP+2.*WO)
      XCOF(4)=3./B+4.*WO/(B*B)+2.*WO/(B*B*OP)+4./(AO*B)
      XCOF(5)=2./(B*B)
      CALL POLRT(XCOF,COF,M,ROOTR,ROOTI,IER)
      WPACT=(ROOTI(1)**2+ROOTR(1)**2)**0.5
      QPACT=(-1.)*WPACT /(2.*ROOTR(1))
      B1=(XCOF(5)*(WPACT**4)-XCOF(3)*(WPACT**2)+XCOF(1))**2
      B2=(XCOF(2)*WPACT-XCOF(4)*(WPACT**3))**2
      A1=(WO*WO/(AO*OP))**2
      A2=((2.*WO/OP-WO*WO/(OP*B))*WPACT)**2
      GAIN=((A1+A2)/(B1+B2))**0.5
      FPACT=WPACT/(2.*3.14159)
      DEVQP=(QPACT-QP)/QP
      DEVFP=(FPACT-FP)/FP
      PRINT4,QP,QPACT,DEVQP,GAIN
    4 FORMAT(4X,*QP=*,F7.1,4X,*QPACT=*,F10.4,4X,*DEVQP=*,F10.4,4X,*GAIN=
     1*,F7.4)
      PRINT 5,FP,FPACT,DEVFP
    5 FORMAT(4X,*FP=*,F12.0,4X,*FPACT=*,F12.2,4X,*DEVFP=*,F14.6)
      PRINT6,(ROOTR(J),ROOTI(J), J=1,4)
    6 FORMAT(4X,*REAL PART=*,E16.7,6X,*IMAG PART=*,E20.7,/)
    1 CONTINUE
    3 CONTINUE
      STOP
      END
```

```
      PROGRAM DESB(INPUT,OUTPUT)
C     * EFFECT OF OP. AMP. IMPERFECTIONS ON DESIGN B *
C     * OP=20 TO 100, FO = 1KHZ TO 10KHZ*
C     *  TYPE 715 OP.AMP. *
      DIMENSION XCOF(5),COF(5),ROOTR(5),ROOTI(5)
      M=4
      B=2.*3.14159*65000000.
      AO=30000.
      DO 3 NQ=25,100,25
      QP=NQ
      DO 1 I=1000,10000,250
      FP=I
      WO=2.*3.14159*FP
      XCOF(1)=WO*WO*(1.+1./AO+1./(AO*QP)+2./(AO*AO)+2./(AO*AO*QP))
      XCOF(2)=WO/QP+WO/AO*(4.+3./QP+4./AO+4.*WO/B+2./(AO*QP))
     1+WO*WO/B*(1.+1./QP+4./(AO*QP))
      XCOF(3)=1.+3./AO+3./(AO*AO)+WO/(AO*B)*(8.+4./QP)+WO/(B*B*QP)*
     1(4.*B*QP+3.*B+2.*WO*   QP+2.*WO)
      XCOF(4)=3./B+4.*WO/(B*B)+2.*WO/(B*B*QP)+4./(AO*B)
      XCOF(5)=2./(B*B)
      CALL POLRT(XCOF,COF,M,ROOTR,ROOTI,IER)
      WPACT=(ROOTI(1)**2+ROOTR(1)**2)**0.5
      QPACT=(-1.)*WPACT /(2.*ROOTR(1))
      B1=(XCOF(5)*(WPACT**4)-XCOF(3)*(WPACT**2)+XCOF(1))**2
      B2=(XCOF(2)*WPACT-XCOF(4)*(WPACT**3))**2
      A1=(WO*WO/(AO*QP))**2
      A2=((2.*WO/QP-WO*WO/(QP*B))*WPACT)**2
      GAIN=((A1+A2)/(B1+B2))**0.5
      FPACT=WPACT/(2.*3.14159)
      DEVQP=(QPACT-QP)/QP
      DEVFP=(FPACT-FP)/FP
      PRINT4,QP,QPACT,DEVQP,GAIN
    4 FORMAT(4X,*QP=*,F7.1,4X,*QPACT=*,F10.4,4X,*DEVQP=*,F10.4,4X,*GAIN=
     1*,F7.4)
      PRINT 5,FP,FPACT,DEVFP
    5 FORMAT(4X,*FP=*,F12.0,4X,*FPACT=*,F12.2,4X,*DEVFP=*,F14.6)
      PRINT6, (ROOTR(J),ROOTI(J), J=1,4)
    6 FORMAT(4X,*REAL PART=*,E16.7,6X,*IMAG PART=*,E20.7,/)
    1 CONTINUE
    3 CONTINUE
      STOP
      END
```